*J. Fluid Mech.* (2020), *vol.* 890, A5. © The Author(s), 2020.
Published by Cambridge University Press
doi:10.1017/jfm.2020.128



# The generation and conservation of vorticity: deforming interfaces and boundaries in two-dimensional flows

**S. J. Terrington[1],†, K. Hourigan[1] and M. C. Thompson[1]**

[1]Fluids Laboratory for Aeronautical and Industrial Research (FLAIR), Department of Mechanical and Aerospace Engineering, Monash University, Melbourne, VIC 3800, Australia

(Received 1 November 2019; revised 21 January 2020; accepted 10 February 2020)

This article presents a revised formulation of the generation and transport of vorticity at generalised fluid–fluid interfaces, substantially extending the work of Brøns *et al.* (*J. Fluid Mech.*, vol. 758, 2014, pp. 63–93). Importantly, the formulation is effectively expressed in terms of the conservation of vorticity, and the latter is shown to hold for arbitrary deformation and normal motion of the interface; previously, vorticity conservation had only been demonstrated for stationary interfaces. The present formulation also affords a simple physical description of the generation of vorticity in incompressible, Newtonian flows: the only mechanism by which vorticity may be generated on an interface is the inviscid relative acceleration of fluid elements on each side of the interface, due to pressure gradients or body forces. Viscous forces act to transfer circulation between the vortex sheet representing the interface slip velocity, and the fluid interior, but do not create vorticity on the interface. Several representative example flows are considered and interpreted under the proposed framework, illustrating the generation, transport and, importantly, the conservation of vorticity within these flows.

**Key words:** vortex interactions

## 1. Introduction

Vorticity, and vortex structures, have long been understood as one of the most important aspects describing a fluid flow (Küchemann 1965; Brøns *et al.* 2014). Many flow structures, including boundary layers, wakes and turbulence, are more easily understood, visualised and interpreted in terms of vorticity, rather than velocity. The power of vorticity dynamics was not lost on Lighthill (1963), who observed that while both vorticity and momentum considerations are able to describe the detailed development of boundary layers, vorticity dynamics is necessary to place the boundary layer in the flow as a whole, and to describe the wake structures formed when the boundary layer separates.

It is well understood that, in incompressible flow, all vorticity has its origins at fluid boundaries (Morton 1984). Despite this, the mechanisms that drive the generation of

† Email address for correspondence: stephen.terrington@monash.edu

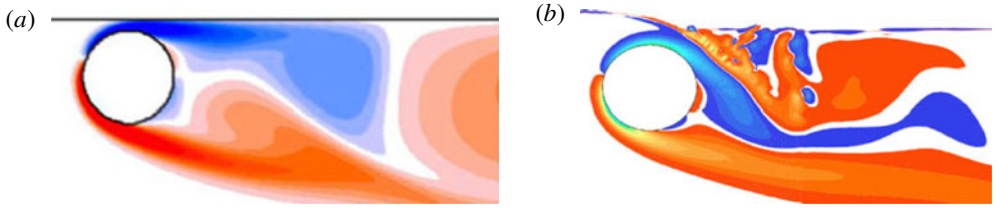


FIGURE 1. Vorticity contours of flow past a cylinder near a free surface, at a Reynolds number of $Re = 180$, and with Froude number and gap-diameter ratios of (*a*) $Fr = 0$ and $G/D = 0.125$ (Brøns *et al.* 2014), and (*b*) $Fr = 0.6$ and $G/D = 0.25$ (Reichl, Hourigan & Thompson 2005). Figures reproduced with permission.

vorticity at fluid boundaries are often poorly understood (Brøns *et al.* 2014), and have been much debated in the literature. Recently, Brøns *et al.* (2014) have presented a formulation of vorticity generation at general fluid–fluid interfaces in two-dimensional flows, including both no-slip and stress-free boundaries. By including the jump in tangential velocity across an interface as part of the total circulation distribution, as an 'interface vortex sheet', they find that vorticity may be generated by a net pressure gradient across the interface, or by normal motion of the interface, generalising Morton's (1984) description of vorticity generation at solid, no-slip boundaries.

Brøns *et al.*'s (2014) formulation enables a description of the conservation of vorticity, providing a unique insight into flow behaviour. In many flow configurations, there is no net external pressure gradient, so that if the boundaries are stationary, the total circulation in the flow is conserved. Vorticity (circulation) may be transferred between the fluid interior and the interface velocity jump, but the area-integrated vorticity remains constant. This description of vorticity generation generalises the work of Lundgren & Koumoutsakos (1999), who had previously described a similar conservation principle for free-surface flows in both two and three dimensions.

The original motivation for Brøns *et al.* (2014) arose from considering the two-dimensional flow past a submerged circular cylinder near a free surface (Sheridan, Lin & Rockwell 1997; Reichl *et al.* 2005; Bozkaya *et al.* 2011), depicted in figure 1. At low Froude numbers, where the interface remains relatively flat, clockwise-oriented vorticity generated on the solid cylinder 'disappears' into the free surface, while at high Froude numbers, where the interface becomes highly curved, a jet of anti-clockwise vorticity streams out of the free surface. This behaviour is easily explained by Brøns *et al.*'s formulation: the zero shear-stress condition provides a Dirichlet boundary condition for vorticity at the free surface, and circulation is exchanged between the interface vortex sheet and fluid elements on the boundary to maintain this condition. For a flat free surface, the zero shear-stress condition requires $\omega = 0$ on the free surface. Any vorticity that diffuses to the interface from the fluid interior disappears into the interface vortex sheet to maintain the shear-free condition, as seen in figure 1(*a*). However, when the interface is curved, the vorticity boundary condition is equivalent to solid-body rotation of fluid elements (Longuet-Higgins 1998). The appearance of anti-clockwise oriented vorticity on the free surface to maintain this condition, demonstrated in figure 1(*b*), is balanced by a change in the interface circulation, so that the total circulation in the flow is conserved. While other descriptions of vorticity generation at free surfaces (Rood 1994*b*; Cresswell & Morton 1995) can explain this behaviour without reference to the interface circulation, these descriptions do not readily generalise to arbitrary fluid–fluid interfaces. Furthermore,

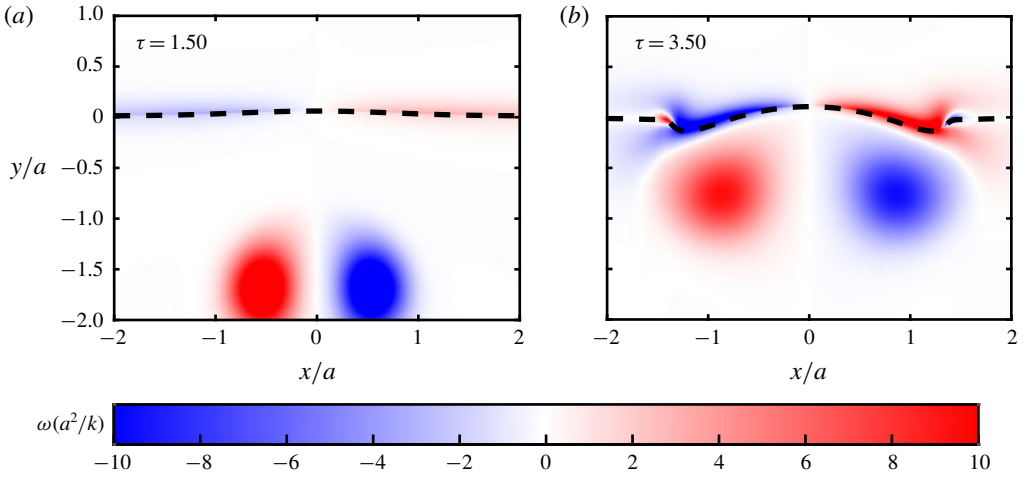


FIGURE 2. Interaction of a vortex pair with a viscous interface, resulting in unsteady deformation of the interface. Such unsteady behaviour is typical of vortex–interface interactions. Here, the Froude number is $Fr = 0.2$, the Reynolds number is $Re = 100$ and the interface density jump is $\rho_2/\rho_1 = 2$. For more details, see § 3.4.

Brøns *et al.* (2014) remark that a description allowing conservation of circulation is beneficial, as conservation of a physical quantity provides a powerful analysis tool.

For this reason, the generation of vorticity due to normal motion of the interface which appears in Brøns *et al.*'s (2014) analysis is problematic. In typical vortex–surface interactions, unsteady motions of the interface are expected, severely limiting the range of flows to which vorticity conservation may be applied. For example, consider the (two-dimensional) interaction between a vortex pair and a free surface (Sarpkaya & Henderson 1984; Ohring & Lugt 1991; Dommermuth 1993), or a viscous fluid–fluid interface as is depicted in figure 2. As the vortex pair approaches the interface, the induced velocity field produces normal motion of the interface, elevating the interface in the region above the vortex pair, and producing a depression, or 'scar', in the immediate neighbourhood of the vortex pair. According to Brøns *et al.*'s (2014) analysis, such normal motion of the interface generates circulation in the interface vortex sheet kinematically, making this description more cumbersome to use than other 'non-conservation' descriptions, at least when applied to actively distorting surfaces.

Furthermore, the surface deformation term proposed by Brøns *et al.* (2014), in their equation (2.19), is not Galilean invariant. Since net circulation is independent of the reference frame, this result is clearly non-physical. Consider, for example, the two-dimensional periodic travelling wave illustrated in figure 3. When viewing this wave from a stationary reference frame, where the mean fluid velocity is zero, significant normal motion of the interface occurs, indicating the generation of circulation. However, the interface is stationary when viewed from a reference frame translating at the wave velocity, suggesting that no circulation is generated. Clearly, the amount of circulation generated cannot be affected by a change in reference frame, and therefore the surface deformation term, in the form proposed by Brøns *et al.* (2014), cannot be a physically distinct source of vorticity.

These issues prompted a review of the vorticity generation terms presented in Brøns *et al.* (2014), where it was found that the derivation contained in that paper

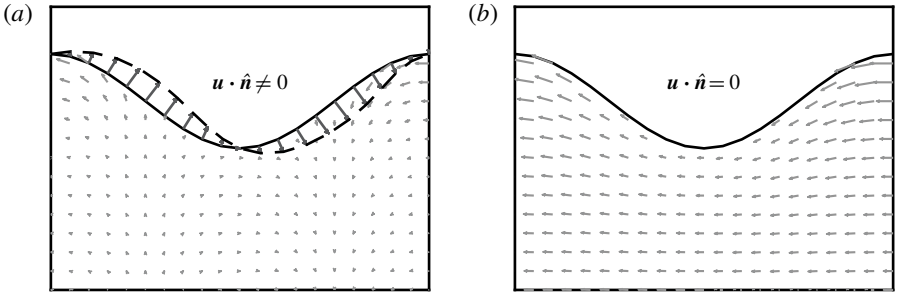


FIGURE 3. Viscous gravity wave viewed from (*a*) a stationary reference frame and (*b*) a moving reference frame. Normal motion of the interface is observed in the stationary reference frame, suggesting the generation of circulation on the interface. However, as the surface is stationary in the moving reference frame, no circulation can be generated.

is not applicable to flows featuring normal motion of the interface. (We remark that Brøns *et al.*'s original formulation remains applicable to flows which feature distorted, but stationary, surfaces, such as the flow depicted in figure 1*b*.) A revised derivation is presented in the present article, which demonstrates that surface deformation (normal motion) is not a direct source of vorticity. Vorticity may be conserved at both stationary and moving interfaces and free surfaces, generalising the findings of Lundgren & Koumoutsakos (1999) to a large variety of interfaces. Furthermore, the present formulation may be interpreted as an extension of Morton's (1984) description of vorticity generation to general interfaces in two-dimensional flows, both stationary and deforming. The only mechanism by which circulation can be generated on an interface is an inviscid relative acceleration between fluid elements on both sides of the interface, by either pressure or body forces. Under the proposed interpretation, viscous forces act to transfer circulation between the interface and the fluid, but do not generate circulation on the interface.

This article is laid out as follows: a brief review of vorticity dynamics on boundaries is presented in the first section. In the second section, a revised formulation of Brøns *et al.*'s (2014) total circulation balance is given. We provide a description of the generation of vorticity at the interface between two generalised incompressible fluids in a two-dimensional flow, which is valid for any tangential boundary conditions on the interface, and may be applied to both solid boundaries and free-surfaces. Application of this general formulation to viscous no-slip interfaces and free surfaces will be discussed in this section. Finally, a range of example flows are considered in the third section, demonstrating the generation, transport and conservation of vorticity and circulation at moving interfaces and free surfaces.

### 1.1. *Preliminary theory*

We now present a brief review of some important aspects of boundary vorticity dynamics. Unless otherwise stated, results in this section apply equally to both two and three-dimensional flows.

Vorticity is defined mathematically as the curl of the velocity field,

$$\boldsymbol{\omega} = \nabla \times \boldsymbol{u}(\boldsymbol{r}, t), \tag{1.1}$$

where $\boldsymbol{u}$ is the fluid velocity at a point $\boldsymbol{r}$ in space, and at time $t$. Physically, vorticity may be understood as twice the mean rotation rate of material lines in the fluid, or,

equivalently, as twice the local angular velocity of a fluid element (Truesdell 1954). Vorticity is related to the circulation through Stokes' theorem,

$$\Gamma = \oint_C \boldsymbol{u} \cdot \mathrm{d}\boldsymbol{l} = \int_S \boldsymbol{\omega} \cdot \mathrm{d}\boldsymbol{S}, \tag{1.2}$$

where $S$ is any surface bounded by a closed contour $C$. In this sense, circulation is a measure of global fluid rotation, and vorticity may be considered as a measure of 'circulation density'.

An evolution equation for the vorticity field – the Helmholtz vorticity equation – is obtained by taking the curl of the Navier–Stokes equations, which, for an incompressible homogeneous fluid, gives

$$\frac{\partial \boldsymbol{\omega}}{\partial t} + (\boldsymbol{u} \cdot \boldsymbol{\nabla})\boldsymbol{\omega} = (\boldsymbol{\omega} \cdot \boldsymbol{\nabla})\boldsymbol{u} + \nu \nabla^2 \boldsymbol{\omega}. \tag{1.3}$$

As discussed by Morton (1984), there is no true vorticity source term in this equation, and hence the source of all vorticity in the flow lies at fluid boundaries. The left-hand side of (1.3) is the material derivative of vorticity, while the first term on the right-hand side represents amplification and rotation of the vorticity vector due to vortex stretching and tilting. While vortex stretching and tilting is an important aspect of three-dimensional flows, the present article is concerned with two-dimensional flows, where this term is equal to zero. The final term represents diffusion of vorticity by viscous forces, which both Lighthill (1963) and Morton (1984) stress should be understood as a consequence of the diffusion of linear momentum.

Lighthill (1963) identifies solid boundaries as sources of vorticity, recognising the boundary vorticity flux,

$$\boldsymbol{\sigma} = \nu \hat{\boldsymbol{n}} \cdot \boldsymbol{\nabla} \boldsymbol{\omega}, \tag{1.4}$$

as the rate at which vorticity enters the fluid from the solid boundary due to viscous diffusion. Here, $\hat{\boldsymbol{n}}$ is the unit normal vector directed out of the fluid domain. Lighthill also recognises that the vorticity flux may be related to the tangential pressure gradient at the surface through the momentum equation. Wu & Wu (1993) extend Lighthill's equation for the vorticity flux to three-dimensional solid boundaries, while Wu (1995) provides the general form of this equation as

$$\boldsymbol{\sigma} = \hat{\boldsymbol{n}} \times \boldsymbol{a} + \hat{\boldsymbol{n}} \times \boldsymbol{\nabla} \left( \frac{p}{\rho} + gz \right) + \nu (\hat{\boldsymbol{n}} \times \boldsymbol{\nabla}) \times \boldsymbol{\omega}, \tag{1.5}$$

where $\boldsymbol{a} = \mathrm{d}\boldsymbol{u}/\mathrm{d}t$ is the fluid acceleration, $p$ is the pressure and $gz$ is the body-force potential.

Equation (1.5) is an expression of the momentum equation, leading Lundgren & Koumoutsakos (1999) to remark that it is not an equation that determines the boundary vorticity flux, but rather an expression for the acceleration of fluid elements on the boundary. The vorticity flux appears in (1.5) in place of the tangential viscous acceleration, and Rood (1994*b*) argues that the boundary vorticity flux is a consequence of this viscous acceleration. We provide the following clarification: since the vorticity field is kinematically linked to the velocity field, the tangential boundary acceleration and the boundary vorticity flux do not represent physically distinct processes. The viscous acceleration of boundary fluid elements is due to the diffusion of linear momentum by viscous stresses; the boundary vorticity flux describes the

effects of the diffusion of linear momentum on the vorticity field. Viscous forces are responsible for both the viscous boundary acceleration and the boundary vorticity flux, and these two effects always occur simultaneously.

While equation (1.5) can be used to determine the rate of vorticity creation on solid boundaries, Morton (1984) remarks that this equation alone does not provide a mechanism for the generation of vorticity. Batchelor (1967), who recognised that the behaviour of vorticity on boundaries must be related to the velocity boundary condition, attributes the creation of vorticity on solid boundaries to the no-slip condition. Morton (1984) provides an alternative description, where vorticity is generated on a solid boundary by the inviscid relative acceleration between the fluid and the solid boundary, by either external acceleration of the solid wall, or by pressure gradients in the fluid. Viscosity, and the no-slip condition, play no role in the generation of vorticity under Morton's interpretation, however, are responsible for the diffusion of vorticity into the fluid once it has been generated. Specifically, circulation, rather than vorticity, is generated on the boundary by the inviscid relative acceleration, and this circulation is then diffused into the fluid by the viscous boundary vorticity flux. Morino (1986) presents a similar inviscid mechanism for the generation of vorticity, while Wu & Wu (1993) and Wu (1995) argue that the vorticity generation process must be a viscous process.

The generation of vorticity at a free surface has been discussed by Longuet-Higgins (1953, 1992, 1998), Batchelor (1967), Lugt (1987), Rood (1994*a*,*b*), Cresswell & Morton (1995), Sarpkaya (1996), Peck & Sigurdson (1998, 1999), Lundgren & Koumoutsakos (1999) and Brøns *et al.* (2014). Tangential vorticity appears spontaneously on the free surface to satisfy the zero shear-stress (stress-free) condition, which requires, on a stationary free surface in a two-dimensional flow,

$$\omega_s = 2\kappa(\boldsymbol{u}\cdot\hat{\boldsymbol{t}}), \tag{1.6}$$

where $\hat{\boldsymbol{t}}$ is the unit tangent vector to the free surface and $\kappa$ is the curvature of the free surface. The unsteady three-dimensional form of this equation is given by Longuet-Higgins (1998) and Peck & Sigurdson (1998). Physically, this condition requires that fluid elements on the boundary rotate with the same angular velocity as the unit normal to the free surface (Peck & Sigurdson 1998), a condition often described as being equivalent to 'solid-body rotation' of boundary fluid elements (Longuet-Higgins 1998).

Vorticity that appears on the free surface can diffuse into the fluid interior along vorticity gradients (Cresswell & Morton 1995), under the action of viscous stresses. The flux of vorticity into or out of the free surface required to enforce the stress-free condition is associated with a tangential viscous acceleration of the surface fluid. Lundgren & Koumoutsakos (1999) interpret this interaction as a transfer of circulation between the fluid and an interface vortex sheet, with conservation of total circulation. The description given by Brøns *et al.* (2014) extends this result to general, albeit stationary, fluid–fluid interfaces in two-dimensional flows.

Wu (1995) investigates the generation of vorticity on no-slip, viscous, fluid–fluid interfaces and finds that the generation mechanism on the interface is a combined viscous–baroclinic effect. Wu identifies two conditions that drive the behaviour of vorticity on the interface: the interface shear-stress balance, which provides a jump condition on vorticity; and the no-slip condition, which gives the vorticity creation rate when combined with the momentum equation. While Brøns *et al.* (2014) identify the net creation rate at no-slip interfaces, the influence of the shear-stress balance on driving the vorticity field across the interface is not discussed. The jump in vorticity across the interface due to the shear-stress balance is also discussed by Dopazo, Lozano & Barreras (2000).

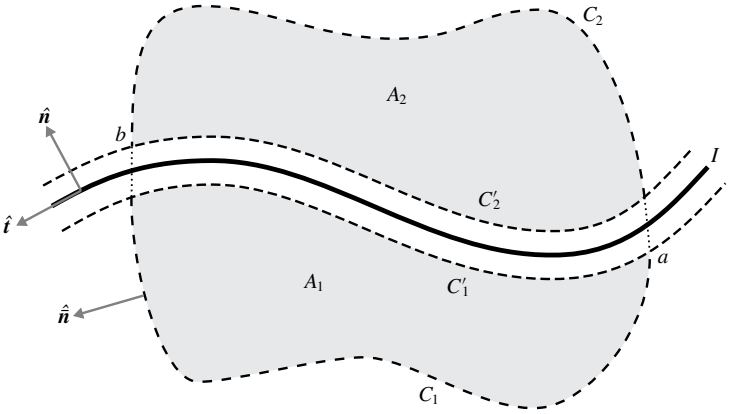


FIGURE 4. Control volumes $A_1$ and $A_2$, sandwiching an interface, $I$, between two fluids. The unit normal and tangent vectors to the interface are denoted $\hat{\boldsymbol{n}}$ and $\hat{\boldsymbol{t}}$, respectively. Each control volume $A_i$ is bounded by two curves; $C_i'$, the portion of the boundary curve coincident with the interface, and $C_i$, the portion of the boundary in the fluid interior. Outward normal vectors to each control volume are denoted by $\hat{\hat{\boldsymbol{n}}}$.

## 2. Integral vorticity balance

In this section, a revised formulation of the total circulation balance for two-dimensional interfacial flows is presented, where it is demonstrated that the only mechanism by which vorticity is generated on an interface is the inviscid relative acceleration of fluid elements on either side of the interface. In contrast with the formulation of Brøns *et al.* (2014), normal motion of the interface does not generate circulation directly.

We first provide a derivation of the general formulation, which is valid for two-dimensional flows of incompressible, Newtonian fluids, with continuity of normal velocity the only boundary condition applied on the interface. In particular, the no-slip condition is not enforced, and the velocity jump across a free-slip interface is included as an 'interface vortex sheet' in the total circulation balance. Following the development of the general theory, application of this formulation to both viscous no-slip interfaces and free surfaces is discussed. While solid boundaries can also be discussed under the present framework, the description is identical to that given by Brøns *et al.* (2014), and will not be examined in this paper.

### 2.1. *Generalised formulation*

Consider the interface between two incompressible fluids in a two-dimensional flow, as depicted in figure 4. In each fluid region $i = 1, 2$ exists a control volume $A_i$, bounded by two curves: $C_i'$ – a portion parallel to the interface, and $C_i$ – the outer boundary. We take the limit as the control-volume boundaries approach the interface, $C_1', C_2' \to I$, and consider a single control volume, $A = A_1 \cup A_2$, bounded by the outer boundary curve $C = C_1 \cup C_2$. The curves $C_1$ and $C_2$ must intersect the interface at the same points, $a$ and $b$, so that $C_1'$ and $C_2'$ coincide with the same portion of the interface. Control volumes (technically control areas, as flow is two-dimensional) are used in preference to material volumes, due to relative sliding of material volumes that would occur when there is a slip velocity on the interface.

Following the notation in Brøns *et al.* (2014), a subscript $\theta_i$ denotes the value of property $\theta$ in fluid $i$, especially on the boundary. Furthermore, $[\![\theta]\!] = \theta_2 - \theta_1$ indicates the jump in $\theta$ across the interface.

The total circulation in $A$ may be written as

$$\Gamma = \oint_C \boldsymbol{u} \cdot \mathrm{d}\boldsymbol{s} = \Gamma_1 + \Gamma_2 + \int_a^b \gamma \, \mathrm{d}s, \tag{2.1}$$

where $\Gamma_i = \oint_{C_i + C_i'} \boldsymbol{u}_i \cdot \mathrm{d}\boldsymbol{s}$ is the circulation contained in $A_i$, and $\gamma = [\![\boldsymbol{u} \cdot \hat{\boldsymbol{t}}]\!]$ is the density of circulation contained in the interface slip velocity, so that $\int_a^b \gamma \, \mathrm{d}s$ is the total circulation contained in the interface due to the slip velocity. The total circulation in the fluid-interface system includes both circulation in the fluid and the interface circulation. It must be stressed that circulation contained in the interface vortex sheet arises from a velocity jump across the interface, and is not a modelling of the vorticity distribution near the interface. The primary motivation for including the interface circulation in this manner is Morton's (1984) description of vorticity generation on solid boundaries, where the slip velocity created by the relative acceleration between fluid elements and the boundary is treated as a net circulation across the boundary. Furthermore, including a slip velocity on the interface allows a general description of vorticity dynamics, applicable to both no-slip and free-slip interfaces.

Using Stokes' theorem (1.2), the circulation in each fluid can be related to the integral of vorticity,

$$\Gamma = \int_{A_1 \cup A_2} \omega \, \mathrm{d}A + \int_a^b \gamma \, \mathrm{d}s. \tag{2.2}$$

Here, $\int_{A_1 \cup A_2} \omega \, \mathrm{d}A$ is shorthand for $\sum_{i=1}^{2} \int_{A_i} \omega_i \, \mathrm{d}A$, and $\omega_i = \boldsymbol{\omega}_i \cdot \hat{\boldsymbol{k}}$ is the scalar vorticity (in two-dimensional flows, vorticity is always normal to the plane of motion, and may be treated as a scalar).

Taking the time derivative of (2.2) yields an expression for the rate of change of circulation,

$$\frac{\mathrm{d}\Gamma}{\mathrm{d}t} = \frac{\mathrm{d}}{\mathrm{d}t} \int_{A_1 \cup A_2} \omega \, \mathrm{d}A + \frac{\mathrm{d}}{\mathrm{d}t} \int_a^b \gamma \, \mathrm{d}s. \tag{2.3}$$

Applying the Reynolds transport theorem to the vorticity terms gives

$$\frac{\mathrm{d}}{\mathrm{d}t} \int_{A_i} \omega \, \mathrm{d}A = \int_{A_i} \frac{\partial \omega}{\partial t} \, \mathrm{d}A + \oint_{C_i \cup C_i'} (\hat{\boldsymbol{n}} \cdot \boldsymbol{v}^b) \omega \, \mathrm{d}s, \tag{2.4}$$

where $\partial\omega/\partial t$ is the time derivative in an Eulerian reference frame, and $\boldsymbol{v}^b$ is the velocity of the control-volume boundary in the Eulerian frame. Using the two-dimensional form of (1.3), and after applying the divergence theorem, this expression becomes

$$\frac{\mathrm{d}}{\mathrm{d}t} \int_{A_i} \omega \, \mathrm{d}A = \int_{C_i} \nu \hat{\hat{\boldsymbol{n}}} \cdot \nabla \omega \, \mathrm{d}s + \int_{C_i'} \nu \hat{\hat{\boldsymbol{n}}} \cdot \nabla \omega \, \mathrm{d}s + \int_{C_i} \hat{\hat{\boldsymbol{n}}} \cdot (\boldsymbol{v}^b - \boldsymbol{u}) \omega \, \mathrm{d}s. \tag{2.5}$$

In addition to the diffusive vorticity flux, an advective flux is also present when a control-volume formulation is used. Note that since $\hat{\boldsymbol{n}} \cdot \boldsymbol{u} = \hat{\boldsymbol{n}} \cdot \boldsymbol{v}^b$ along the interface (the control volume remains attached to the interface), there is no advective flux into or out of the interface.

Substituting the expression in (2.5) into (2.3) yields

$$\frac{\mathrm{d}\Gamma}{\mathrm{d}t} = \oint_C \nu\hat{\hat{\boldsymbol{n}}}\cdot\boldsymbol{\nabla}\omega\,\mathrm{d}s + \oint_C \hat{\hat{\boldsymbol{n}}}\cdot(\boldsymbol{v}^b-\boldsymbol{u})\omega\,\mathrm{d}s + \int_a^b(\sigma_1+\sigma_2)\,\mathrm{d}s + \frac{\mathrm{d}}{\mathrm{d}t}\int_a^b \gamma\,\mathrm{d}s, \tag{2.6}$$

where $\sigma_1 = \nu\hat{\boldsymbol{n}}\cdot\boldsymbol{\nabla}\omega_1$ and $\sigma_2 = -\nu\hat{\boldsymbol{n}}\cdot\boldsymbol{\nabla}\omega_2$ are the diffusive fluxes of vorticity from the interface into fluids 1 and 2, respectively. Note that this expression is equivalent to (2.6) in Brøns *et al.* (2014), apart from the inclusion of advection terms due to the use of control volumes rather than material volumes.

2.1.1. *Rate of change of interface circulation*

We now turn our attention to the rate of change of interface circulation. Brøns *et al.* (2014) had assumed the total derivative could be taken inside the integral as

$$\frac{\mathrm{d}}{\mathrm{d}t}\int_a^b \gamma\,\mathrm{d}s = \int_a^b \frac{\mathrm{d}\gamma}{\mathrm{d}t}\,\mathrm{d}s. \tag{2.7}$$

This assumption is problematic for the following reasons. First, the order of differentiation and integration cannot, in general, be interchanged. Second, the material derivative of interface circulation is not well defined, since velocity is discontinuous across the interface (Lundgren & Koumoutsakos 1999). Instead, we express the interface circulation as the sum of two line integrals,

$$\frac{\mathrm{d}}{\mathrm{d}t}\int_a^b \gamma\,\mathrm{d}s = \frac{\mathrm{d}}{\mathrm{d}t}\int_a^b \boldsymbol{u}_2\cdot\mathrm{d}\boldsymbol{s} - \frac{\mathrm{d}}{\mathrm{d}t}\int_a^b \boldsymbol{u}_1\cdot\mathrm{d}\boldsymbol{s}. \tag{2.8}$$

In order to evaluate these integrals, the interface is parametrised as $\boldsymbol{y}(s', t)$, where $s'$ is such that the bounds of integration, $s'_a$ and $s'_b$, are constant. This differs from $s$, the arc-length parameter, since the length of the curve $a-b$ may not remain constant. Points of constant $s'$, $\boldsymbol{y}(s' = \text{const.}, t)$, are neither material points, nor fixed Eulerian reference points, but arbitrary reference points which move along the interface with the control-volume boundary, at a velocity $\boldsymbol{v}^b$. Note that while the normal component of $\boldsymbol{v}^b$ is equal to the normal velocity at the interface, the tangential component is arbitrary, except at the endpoints, $a$ and $b$.

Under this parametrisation, the bounds of integration are constant, and the derivative may be taken inside the integral,

$$\frac{\mathrm{d}}{\mathrm{d}t}\int_a^b \boldsymbol{u}\cdot\hat{\boldsymbol{t}}\,\mathrm{d}s = \frac{\mathrm{d}}{\mathrm{d}t}\int_a^b \boldsymbol{u}(\boldsymbol{y},t)\cdot\frac{\partial\boldsymbol{y}}{\partial s'}\,\mathrm{d}s' = \int_a^b \left.\frac{\partial\boldsymbol{u}}{\partial t}\right|_{s'}\cdot\frac{\partial\boldsymbol{y}}{\partial s'}\,\mathrm{d}s' + \int_a^b \boldsymbol{u}\cdot\frac{\partial^2\boldsymbol{y}}{\partial t\partial s'}\,\mathrm{d}s', \tag{2.9}$$

where the subscript $s'$ indicates that partial time derivatives are taken at a constant $s'$. Since $\partial\boldsymbol{y}/\partial t = \boldsymbol{v}^b$, this expression becomes

$$\frac{\mathrm{d}}{\mathrm{d}t}\int_a^b \boldsymbol{u}\cdot\mathrm{d}\boldsymbol{s} = \int_a^b \left.\frac{\partial\boldsymbol{u}}{\partial t}\right|_{s'}\cdot\hat{\boldsymbol{t}}\,\mathrm{d}s + \int_a^b \boldsymbol{u}\cdot\frac{\partial\boldsymbol{v}^b}{\partial s}\,\mathrm{d}s. \tag{2.10}$$

The partial derivative for a constant $s'$ can be related to the material derivative through ALE (arbitrary Lagrangian–Eulerian) theory (Donea *et al.* 2004), which is typically applied in numerical methods,

$$\left.\frac{\partial\boldsymbol{u}}{\partial t}\right|_{s'} = \frac{\mathrm{d}\boldsymbol{u}}{\mathrm{d}t} - (\boldsymbol{u}-\boldsymbol{v}^b)\cdot\boldsymbol{\nabla}\boldsymbol{u}. \tag{2.11}$$

Since $(\boldsymbol{u}-\boldsymbol{v}^b)\cdot\hat{\boldsymbol{n}}=0$, we can express the tangential component of this equation as

$$\left.\frac{\partial \boldsymbol{u}}{\partial t}\right|_{s'}\cdot\hat{\boldsymbol{t}}=\frac{\mathrm{d}\boldsymbol{u}}{\mathrm{d}t}\cdot\hat{\boldsymbol{t}}-(\boldsymbol{u}-\boldsymbol{v}^b)\cdot\frac{\partial \boldsymbol{u}}{\partial s}. \tag{2.12}$$

On substituting this result into (2.10), one obtains

$$\frac{\mathrm{d}}{\mathrm{d}t}\int_a^b \boldsymbol{u}\cdot\mathrm{d}\boldsymbol{s}=\int_a^b\frac{\mathrm{d}\boldsymbol{u}}{\mathrm{d}t}\cdot\mathrm{d}\boldsymbol{s}-\int_a^b(\boldsymbol{u}-\boldsymbol{v}^b)\cdot\frac{\partial \boldsymbol{u}}{\partial s}\,\mathrm{d}s+\int_a^b\boldsymbol{u}\cdot\frac{\partial \boldsymbol{v}^b}{\partial s}\,\mathrm{d}s. \tag{2.13}$$

The term containing $\mathrm{d}\boldsymbol{u}/\mathrm{d}t$ represents changes to the integral due to acceleration of the surface fluid, the second term represents the advective transport of tangential velocity (momentum) along the interface, while the final term represents the effects of variations in the length of the integration curve.

Substituting the result of (2.13) into (2.8), one obtains

$$\begin{aligned}\frac{\mathrm{d}}{\mathrm{d}t}\int_a^b\gamma\,\mathrm{d}s=&\int_a^b\left(\frac{\mathrm{d}\boldsymbol{u}_2}{\mathrm{d}t}-\frac{\mathrm{d}\boldsymbol{u}_1}{\mathrm{d}t}\right)\cdot\hat{\boldsymbol{t}}\,\mathrm{d}s+\int_a^b\left[(\boldsymbol{v}^b-\boldsymbol{u}_2)\cdot\frac{\partial \boldsymbol{u}_2}{\partial s}-(\boldsymbol{v}^b-\boldsymbol{u}_1)\cdot\frac{\partial \boldsymbol{u}_1}{\partial s}\right]\mathrm{d}s\\&+\int_a^b\left[\boldsymbol{u}_2\cdot\frac{\partial \boldsymbol{v}^b}{\partial s}-\boldsymbol{u}_1\cdot\frac{\partial \boldsymbol{v}^b}{\partial s}\right]\mathrm{d}s.\end{aligned} \tag{2.14}$$

Using the product rule, the various terms under the last two integrals may be written

$$\frac{\partial}{\partial s}(\boldsymbol{v}^b\cdot(\boldsymbol{u}_2-\boldsymbol{u}_1))-\frac{\partial}{\partial s}\left(\frac{1}{2}\boldsymbol{u}_2\cdot\boldsymbol{u}_2-\frac{1}{2}\boldsymbol{u}_1\cdot\boldsymbol{u}_1\right). \tag{2.15}$$

Furthermore, since $\boldsymbol{u}_1\cdot\hat{\boldsymbol{n}}=\boldsymbol{u}_2\cdot\hat{\boldsymbol{n}}=\boldsymbol{v}^b\cdot\hat{\boldsymbol{n}}$, this expression is written succinctly as

$$\frac{\partial}{\partial s}(\gamma\boldsymbol{v}^b\cdot\hat{\boldsymbol{t}})-\frac{\partial}{\partial s}\left[\!\!\left[\frac{1}{2}(\boldsymbol{u}\cdot\hat{\boldsymbol{t}})^2\right]\!\!\right], \tag{2.16}$$

where we remind the reader that double square brackets $[\![\ ]\!]$ indicate the jump in some quantity across the interface.

Substituting this expression into (2.14) gives

$$\frac{\mathrm{d}}{\mathrm{d}t}\int_a^b\gamma\,\mathrm{d}s=\int_a^b\left[\!\!\left[\frac{\mathrm{d}\boldsymbol{u}}{\mathrm{d}t}\right]\!\!\right]\cdot\hat{\boldsymbol{t}}\,\mathrm{d}s+\gamma(\boldsymbol{v}^b\cdot\hat{\boldsymbol{t}})|_b-\gamma(\boldsymbol{v}^b\cdot\hat{\boldsymbol{t}})|_a+\frac{1}{2}[\![(\boldsymbol{u}\cdot\hat{\boldsymbol{t}})^2]\!]_a-\frac{1}{2}[\![(\boldsymbol{u}\cdot\hat{\boldsymbol{t}})^2]\!]_b. \tag{2.17}$$

The first term on the right-hand side of (2.17) represents the change in interface circulation due to the relative acceleration between fluid elements on both sides of the interface. Terms involving $\gamma(\boldsymbol{v}^b\cdot\hat{\boldsymbol{t}})$ represent the effects of translation and stretching of the curve $a-b$ along the interface, while the $[\![(\boldsymbol{u}\cdot\hat{\boldsymbol{t}})^2]\!]$ terms represent the change in interface circulation due to a difference in advective transport of tangential velocity (momentum) on both sides of the interface. These effects can be considered as the transport of circulation along the interface, either due to tangential motion of the control-volume boundary, or due to advection of tangential momentum, and do not contribute to the generation of interface circulation. Interface circulation may only be generated by a relative acceleration between fluid elements on each side of the interface.

2.1.2. *Vorticity flux and the boundary acceleration*

The boundary vorticity flux may be related to the boundary acceleration through the momentum equation. The two-dimensional equivalent of (1.5) is (see Lundgren & Koumoutsakos 1999; Brøns *et al.* 2014),

$$\sigma_1 = \frac{\mathrm{d}\boldsymbol{u}_1}{\mathrm{d}t}\cdot\hat{\boldsymbol{t}} + \frac{1}{\rho_1}\frac{\partial p_1}{\partial s} - \boldsymbol{g}_1\cdot\hat{\boldsymbol{t}}, \tag{2.18a}$$

$$\sigma_2 = -\frac{\mathrm{d}\boldsymbol{u}_2}{\mathrm{d}t}\cdot\hat{\boldsymbol{t}} - \frac{1}{\rho_2}\frac{\partial p_2}{\partial s} + \boldsymbol{g}_2\cdot\hat{\boldsymbol{t}}, \tag{2.18b}$$

where the orientation of $\hat{\boldsymbol{n}}$ and $\hat{\boldsymbol{t}}$ has been taken into account in (2.18*b*). Note that the pressure ($p$) and body forces ($\boldsymbol{g}$) do not individually contribute to the vorticity flux, but rather the vorticity flux is proportional to the viscous acceleration, and is in fact driven by viscous stresses in the fluid. Equations (2.18*a*) and (2.18*b*), may be combined to yield an expression for the net vorticity flux out of the interface,

$$\sigma_1 + \sigma_2 = -\left[\!\!\left[\frac{\mathrm{d}\boldsymbol{u}}{\mathrm{d}t}\right]\!\!\right]\cdot\hat{\boldsymbol{t}} - \frac{\partial}{\partial s}\left[\!\!\left[\frac{p}{\rho}\right]\!\!\right] - \frac{\partial}{\partial s}[\![\Phi_g]\!], \tag{2.19}$$

where $\Phi_g$ is the body-force potential, $\boldsymbol{g} = -\nabla\Phi_g$. Note we are assuming a conservative body force; non-conservative body forces introduce an additional source term in (1.3).

Equation (2.19) expresses the fact that the net vorticity flux out of the interface is equal to the difference in viscous acceleration of fluid elements on each side of the interface. As an expression of the momentum equation, this equation should be recast as a force balance,

$$\left[\!\!\left[\frac{\mathrm{d}\boldsymbol{u}}{\mathrm{d}t}\right]\!\!\right]\cdot\hat{\boldsymbol{t}} = -(\sigma_1+\sigma_2) - \frac{\partial}{\partial s}\left[\!\!\left[\frac{p}{\rho}\right]\!\!\right] - \frac{\partial}{\partial s}[\![\Phi_g]\!], \tag{2.20}$$

demonstrating that the relative acceleration of fluid elements on each side of the interface includes contributions from the viscous forces, accompanied by a flux of vorticity into the fluid, and the inviscid pressure and body forces.

This result may be substituted into (2.17), to give

$$\begin{aligned}\frac{\mathrm{d}}{\mathrm{d}t}\int_a^b \gamma\,\mathrm{d}s \;=\; &-\int_a^b(\sigma_1+\sigma_2)\,\mathrm{d}s - \left[\!\!\left[\frac{p}{\rho}\right]\!\!\right]_b + \left[\!\!\left[\frac{p}{\rho}\right]\!\!\right]_a - [\![\Phi_g]\!]_b + [\![\Phi_g]\!]_a \\ &+\gamma(\boldsymbol{v}^b\cdot\hat{\boldsymbol{t}})|_b - \gamma(\boldsymbol{v}^b\cdot\hat{\boldsymbol{t}})|_a + \frac{1}{2}[\![(\boldsymbol{u}\cdot\hat{\boldsymbol{t}})^2]\!]_a - \frac{1}{2}[\![(\boldsymbol{u}\cdot\hat{\boldsymbol{t}})^2]\!]_b.\end{aligned} \tag{2.21}$$

Interface circulation is generated by the relative acceleration of fluid elements on both sides of the interface. This may be due to inviscid forces (pressure or body forces), or due to viscous forces. However, the viscous acceleration of the boundary is associated with a flux of vorticity into the main body of the fluid, so that no net circulation is generated by viscous effects. When equation (2.21) is substituted into the expression for the rate of change of total circulation (2.6),

$$\begin{aligned}\frac{\mathrm{d}\Gamma}{\mathrm{d}t} \;=\; &\oint_C \nu\hat{\hat{\boldsymbol{n}}}\cdot\nabla\omega\,\mathrm{d}s + \oint_C \hat{\hat{\boldsymbol{n}}}\cdot(\boldsymbol{v}^b-\boldsymbol{u})\omega\,\mathrm{d}s - \left[\!\!\left[\frac{p}{\rho}\right]\!\!\right]_b + \left[\!\!\left[\frac{p}{\rho}\right]\!\!\right]_a - [\![\Phi_g]\!]_b + [\![\Phi_g]\!]_a \\ &+\gamma(\boldsymbol{v}^b\cdot\hat{\boldsymbol{t}})|_b - \gamma(\boldsymbol{v}^b\cdot\hat{\boldsymbol{t}})|_a + \frac{1}{2}[\![(\boldsymbol{u}\cdot\hat{\boldsymbol{t}})^2]\!]_a - \frac{1}{2}[\![(\boldsymbol{u}\cdot\hat{\boldsymbol{t}})^2]\!]_b,\end{aligned} \tag{2.22}$$

terms related to the viscous acceleration/vorticity flux on the interface disappear, confirming that viscous effects do not generate a net circulation on the interface. The transport terms in (2.22) indicate that vorticity may enter or exit the control volume by diffusion and advection of vorticity across the outer boundary, or by the advective transfer of circulation along the interface. These effects do not generate circulation, but merely redistribute it throughout the flow.

#### 2.1.3. *Summary of the general formulation*

Equations (2.21) and (2.22) provide a complete description of the generation of circulation at general interfaces in two-dimensional flows. Circulation is generated in the interface by the inviscid relative acceleration of fluid elements on either side of the interface, by either pressure gradients or body forces. Viscous forces transfer circulation between the interface vortex sheet and the fluid interior, but do not generate a net circulation across the interface. This description may be viewed as an extension of Morton's (1984) theory of vorticity generation at solid boundaries: at solid boundaries vorticity (circulation) is generated by the inviscid relative acceleration between the solid boundary and the fluid, and viscous effects are only responsible for the diffusion of the created vorticity away from the wall.

### 2.2. *Conservation of circulation*

Both Lundgren & Koumoutsakos (1999) and Brøns *et al.* (2014) observe that in many cases, far field boundary conditions will be such that there is no net generation of circulation along the interface. When there is no net external pressure gradient or body force ($[\![p/\rho]\!]_b = [\![p/\rho]\!]_a$ and $[\![\Phi_g]\!]_b = [\![\Phi_g]\!]_a$), the net circulation generated on the interface is zero, and circulation is conserved in the sense that total circulation may change only by the flux of circulation out of the control-volume boundary. If the outer boundary extends to an undisturbed far field, then no loss of circulation occurs through the control-volume boundary, and total circulation in $A$ is constant,

$$\Gamma = \int_A \omega \,\mathrm{d}A + \int_a^b \gamma \,\mathrm{d}s = \text{const.} \tag{2.23}$$

Circulation may be transferred between the interface and the two fluids, however, the total circulation remains constant.

It is important to note that this conservation principle is a global statement, and local generation on the interface is likely to occur in many cases where total circulation is conserved – generation of circulation on one section of the interface is balanced by generation of an equivalent amount of opposite-signed circulation elsewhere on the interface. This may lead to the appearance of vortical motion in initially irrotational flows, even when the boundary conditions do not provide an influx of vorticity. The growth of a Rayleigh–Taylor instability, for example, is associated with the generation of vorticity by pressure gradients along the interface. The absence of a net pressure gradient along the boundary does not imply that this flow cannot exist, for local pressure gradients generate both positive and negative circulation, with the total circulation remaining equal to zero.

Importantly, the surface deformation term in Brøns *et al.*'s (2014) equation (2.18) does not appear in the present formulation, so conservation of circulation is not restricted to flows with stationary boundaries. The description of vorticity generation and conservation presented by Brøns *et al.* remains valid for flows featuring stationary

interfaces, since the problematic surface deformation term is equal to zero. The present formulation demonstrates that this description extends to deforming interfaces, without the kinematic generation of circulation by normal motion of the interface.

We should, at this point, return to Brøns *et al.*'s (2014) analysis of the flow past a cylinder near a free surface, to determine whether their findings hold under the revised formulation. Their conclusions in regard to the generation and conservation of vorticity under a flat free surface (their § 4.1) are unchanged, as the problematic normal motion term plays no role. Brøns *et al.* also consider deforming interfaces in their § 4.2, including cases where normal motion of the interface is likely to occur. However, their discussion of these flows is centred around the appearance of vorticity on a curved free surface, which is unchanged under the revised formulation. No mention of either the conservation of vorticity, or the generation of circulation by normal motion of the free surface, is made in the discussion of the flow featured in their figure 17 – our revised formulation demonstrates that no circulation is generated on the free surface, and the conservation of circulation extends to this flow. The 'detached jet' wake state, featured in our figure 1(*b*), and in Brøns *et al.*'s figure 18, features a nearly stationary (quiescent) surface (Sheridan *et al.* 1997). Brøns *et al.* invoke the conservation of circulation in their analysis of this flow, implicitly assuming disturbances of the interface to be negligible. Our revised formulation demonstrates that this analysis holds, even when unsteady motion of the interface occurs, as surface deformation is not a source of circulation.

### 2.3. *No-slip viscous interfaces*

The generation of vorticity at no-slip viscous fluid–fluid interfaces is discussed in this section. For such interfaces, two additional boundary conditions – the no-slip condition, and continuity of shear stress – are applied to the interface, in addition to the continuity of normal velocity. Wu (1995) has presented a description of the generation and behaviour of vorticity on such interfaces, however, it may be useful to investigate these conditions under the present framework. Brøns *et al.* (2014) notes that both solid boundaries and free surfaces can be interpreted as limiting cases of the no-slip interface, the former as $\nu_2 \to \infty$ and the latter as $\nu_2,\ \rho_2 \to 0$, so that viscous no-slip interfaces remain a generalisation of most interfaces and boundaries encountered in fluid dynamics.

The no-slip condition requires that no interface circulation can exist. For $\gamma = 0$, the circulation balance in (2.22) reduces to

$$\begin{aligned}\frac{\mathrm{d}\Gamma}{\mathrm{d}t} &= \frac{\mathrm{d}}{\mathrm{d}t}\int_A \omega\,\mathrm{d}A = \oint_C \nu\hat{\hat{\boldsymbol{n}}}\cdot\boldsymbol{\nabla}\omega\,\mathrm{d}s + \oint_C \hat{\hat{\boldsymbol{n}}}\cdot(\boldsymbol{v}^b - \boldsymbol{u})\omega\,\mathrm{d}s \\ &\quad - \left[\!\!\left[\frac{p}{\rho}\right]\!\!\right]_b + \left[\!\!\left[\frac{p}{\rho}\right]\!\!\right]_a - [\![\Phi_g]\!]_b + [\![\Phi_g]\!]_a. \end{aligned} \tag{2.24}$$

Once again, viscosity does not appear in the vorticity generation terms, and circulation may only be generated on the interface by pressure and body forces.

Applying the no-slip condition to (2.19) gives an expression for the net vorticity flux out of the interface,

$$\sigma_1 + \sigma_2 = -\frac{\partial}{\partial s}\left[\!\!\left[\frac{p}{\rho}\right]\!\!\right] - \frac{\partial}{\partial s}[\![\Phi_g]\!]. \tag{2.25}$$

Following the discussion of (2.22), this equation represents the local vorticity generation rate on the interface due to the inviscid relative acceleration of fluid elements on either side of the interface. This 'inviscid' relative acceleration is the acceleration that would occur if only the inviscid pressure and body forces were applied. Viscous forces oppose this relative acceleration, ensuring the no-slip condition is satisfied. These viscous forces produce a flux of vorticity into the fluid interior, so that all circulation generated by the inviscid mechanism appears as a boundary flux on the interface.

Conceptually, this description is similar to some fractional step algorithms used in numerical solution of the Navier–Stokes equations, where the 'viscous' and 'pressure' velocity updates are artificially decoupled. Lighthill (1963), for example, describes how the amount of vorticity generated on a solid boundary during a short time interval may be ascertained by first considering an 'inviscid' update of the velocity field, where the viscous diffusion of vorticity is ignored. A slip velocity typically appears on the boundary during the pressure update (i.e. the inviscid generation of circulation), which is eliminated during the viscous substep, along with the diffusion of vorticity into the fluid interior.

Wu (1995) has argued that the vorticity generation mechanism on no-slip interfaces must be a viscous effect, since the no-slip condition is assumed in (2.25). Indeed, for no-slip interfaces, one could consider the viscous torques applied to boundary fluid elements as responsible for the generation of vorticity. However, if the no-slip condition does not apply, equations (2.21) and (2.22) demonstrate that the amount of circulation generated does not depend on either viscosity or the no-slip condition, so long as the 'interface circulation' is included in the total circulation balance.

Wu & Wu (1993) argue that as vorticity corresponds to rotation of fluid elements, the velocity jump across a free-slip boundary does not represent a sheet of vorticity on the interface. Under their description, vorticity is not generated by the 'inviscid relative acceleration', but by viscous forces which drive the boundary vorticity flux. The 'interface circulation' presented here is not vorticity carried by rotating fluid elements, but rather a circulation contained in the velocity jump between boundary fluid elements. This is included in the total circulation balance, as it allows the boundary vorticity flux to be described as a conservative process, transferring circulation between the interface vortex sheet and vorticity in the fluid interior. Our description of vorticity dynamics is further justified by the Biot–Savart integral, where the 'interface vortex sheet' is necessary to describe a velocity jump across the interface (Morino 1986).

The form of (2.24) indicates that the conditions required for conservation of circulation are the same as for the general interface. If there is no net external pressure gradient or body force, then the total circulation generated at the interface is zero. Circulation may be transferred across the interface, and local generation of circulation may occur if balanced by generation of opposite-sign vorticity elsewhere. If the outer control-volume boundary is in an undisturbed free stream, so that no vorticity diffuses through the control-volume boundary, then the total circulation within the control volume remains constant. Normal motion and deformation of the interface do not appear in the total circulation balance, and have no direct effect on the conservation of circulation.

While the net vorticity flux is determined by the inviscid relative acceleration and the no-slip condition, this does not determine the values of the individual vorticity fluxes $\sigma_1$ and $\sigma_2$. Expressions such as (2.18*a*) and (2.18*b*), or the integral equivalents, such as (2.26) in Brøns *et al.* (2014), are not useful here, since the

tangential acceleration of the boundary is not determined by the no-slip condition alone. For viscous interfaces, the shear-stress balance is necessary to fully determine the acceleration of the interface, and hence, the vorticity fluxes. Wu (1995) finds that the shear-stress balance constrains the jump in tangential vorticity across the interface. For a two-dimensional flow, this relationship may be expressed as

$$[\![\mu\omega]\!] = [\![\mu]\!] \left( 2\kappa(\boldsymbol{u}\cdot\hat{\boldsymbol{t}}) - 2\frac{\partial}{\partial s}(\boldsymbol{u}\cdot\hat{\boldsymbol{n}}) \right). \tag{2.26}$$

The underlying physics behind this condition can be understood more clearly when the expression is written as

$$\frac{\mu_2}{\mu_1} = \frac{\tau_w/\mu_1}{\tau_w/\mu_2} = \frac{\omega_1 - \left[ 2\kappa(\boldsymbol{u}\cdot\hat{\boldsymbol{t}}) - 2\dfrac{\partial}{\partial s}(\boldsymbol{u}\cdot\hat{\boldsymbol{n}}) \right]}{\omega_2 - \left[ 2\kappa(\boldsymbol{u}\cdot\hat{\boldsymbol{t}}) - 2\dfrac{\partial}{\partial s}(\boldsymbol{u}\cdot\hat{\boldsymbol{n}}) \right]}, \tag{2.27}$$

where $\tau_w = \mu_i(\hat{\boldsymbol{n}}\cdot\nabla\boldsymbol{u}_i\cdot\hat{\boldsymbol{t}} + \hat{\boldsymbol{t}}\cdot\nabla\boldsymbol{u}_i\cdot\hat{\boldsymbol{n}})$ is the tangential shear stress on the interface. The term $2\kappa(\boldsymbol{u}\cdot\hat{\boldsymbol{t}}) - 2\partial(\boldsymbol{u}\cdot\hat{\boldsymbol{n}})/\partial s = 2\hat{\boldsymbol{t}}\cdot\mathrm{d}\hat{\boldsymbol{n}}/\mathrm{d}t$ is twice the angular velocity of the unit normal vector of a fluid element on the interface (Peck & Sigurdson 1998), so that we can consider a decomposition of the boundary vorticity into two components,

$$\omega_i = \omega_{\tau,i} + \omega_r, \tag{2.28a}$$

$$\omega_{\tau,i} = \tau_w/\mu_i, \tag{2.28b}$$

$$\omega_r = 2\kappa(\boldsymbol{u}\cdot\hat{\boldsymbol{t}}) - 2\frac{\partial}{\partial s}(\boldsymbol{u}\cdot\hat{\boldsymbol{n}}). \tag{2.28c}$$

The parameter $\omega_r$ shall be termed the 'rotational vorticity', and is equivalent to solid-body rotation of a boundary fluid element. The $2\kappa(\boldsymbol{u}\cdot\hat{\boldsymbol{t}})$ term in $\omega_r$ indicates rotation of fluid elements as they follow the curvature of the interface, while the $\partial(\boldsymbol{u}\cdot\hat{\boldsymbol{n}})/\partial s$ term indicates rotation of fluid elements as the interface rotates. Importantly, these two terms are not independent of the reference frame, and thus should not be considered separate effects. The rotational component of vorticity does not contribute to the interface shear stress.

The shearing vorticity, $\omega_{\tau,i}$, is the component of vorticity which produces a shear stress on the interface. Equation (2.27) indicates that total vorticity must be distributed across the interface by the boundary fluxes in a manner that ensures the shearing vorticity is balanced in proportion to the ratio of dynamic viscosity. This condition applies to vorticity generated on the interface, as well as vorticity which diffuses to the interface from the fluid interior. The shear-stress balance may also drive the transfer of vorticity across the interface, even when the local generation rate is zero.

Continuity of normal stresses across the interface is a final boundary condition that must be considered for viscous interfaces. This condition can be expressed in terms of the jump in pressure across the interface (Brøns *et al.* 2014),

$$[\![p]\!] = -2\left[\!\!\left[ \mu\left( \frac{\partial}{\partial s}(\boldsymbol{u}\cdot\hat{\boldsymbol{t}}) + \kappa(\boldsymbol{u}\cdot\hat{\boldsymbol{n}}) \right) \right]\!\!\right] - T\kappa, \tag{2.29}$$

where $T$ is the interface surface tension, and $\kappa$ the curvature of the interface. Note that the $\boldsymbol{u}\cdot\hat{\boldsymbol{n}}$ term was inadvertently cancelled by Brøns *et al.* (2014) in their

equation (2.15). Although $\boldsymbol{u}_1 \cdot \hat{\boldsymbol{n}} = \boldsymbol{u}_2 \cdot \hat{\boldsymbol{n}}$, the term $[\![\mu(\boldsymbol{u} \cdot \hat{\boldsymbol{n}})]\!]$ does not vanish in general. When the no-slip condition is enforced, the jump in pressure is given by

$$[\![p]\!] = -2[\![\mu]\!] \left( \frac{\partial}{\partial s}(\boldsymbol{u} \cdot \hat{\boldsymbol{t}}) + \kappa(\boldsymbol{u} \cdot \hat{\boldsymbol{n}}) \right) - T\kappa. \tag{2.30}$$

This can be recast in terms of the pressure generation term (Brøns *et al.* 2014),

$$\frac{\partial}{\partial s}\left[\!\left[\frac{p}{\rho}\right]\!\right] = -2\frac{[\![\mu]\!]}{\rho_2}\left( \frac{\partial^2}{\partial s^2}(\boldsymbol{u} \cdot \hat{\boldsymbol{t}}) + \frac{\partial}{\partial s}(\kappa(\boldsymbol{u} \cdot \hat{\boldsymbol{n}})) \right) - \frac{1}{\rho_2}\frac{\partial}{\partial s}(T\kappa) + \left[\!\left[\frac{1}{\rho}\right]\!\right]\frac{\partial p_1}{\partial s}. \tag{2.31}$$

This expression indicates three factors which may influence generation of vorticity by pressure gradients. The final term, $[\![1/\rho]\!]\partial p_1/\partial s$, is due to the difference in inertia of fluid elements across the interface. Even if the pressure gradient is equal in both fluids, pressure forces still act to drive an inviscid relative acceleration as the less dense fluid will experience a larger acceleration. The remaining terms represent the effects of a jump in pressure across the interface. Viscous stresses and the surface tension force do not directly generate circulation, however, these effects can cause a jump in the pressure gradient across the interface, and this can induce an inviscid relative acceleration. Interface circulation is then generated in the usual manner.

In general, interfaces may be contaminated by surfactants, and the surface tension coefficient will not be constant along the interface (Sarpkaya 1996). Peck & Sigurdson (1998) provide a modified version of the interface stress balance, including the effects of both a finite density surface film and gradients in surface tension. For contaminated interfaces, these effects need to be included in (2.27) and (2.29). Surfactants and surface tension are only indirectly responsible for the generation of vorticity on viscous interfaces, through the normal and shear-stress boundary conditions, and will not be considered in the example flows treated in § 3.

### 2.4. *Free surface*

The free-surface approximation is often used to describe idealised water–air interfaces, where it is assumed, due to the low density and viscosity of air, that the upper fluid does not exert any stress on the lower fluid. In this section, the generation of vorticity in a range of free-surface models is investigated using our general formulation: the zero-density free-surface limit, the inviscid upper fluid model of Lundgren & Koumoutsakos (1999), and a technical free surface.

Wu (1995) considers the conditions for which a viscous interface may be approximated by a free surface, requiring that the upper fluid have negligible density and both negligible kinematic and dynamic viscosity compared to the lower fluid. Unfortunately, the kinematic viscosity of air is greater than that of water, and air–water interfaces cannot be considered free surfaces in this manner.

Here, we take the limit as $\rho_2 \to 0$ and $\mu_2 \to 0$, while keeping $\nu_2$ constant (but not equal to zero), as an approximation of air–water interfaces. From the momentum equation in the upper fluid,

$$\frac{\mathrm{d}\boldsymbol{u}_2}{\mathrm{d}t} = -\frac{1}{\rho_2}\frac{\partial p_2}{\partial s} + \nu\nabla^2\boldsymbol{u}_2 + \boldsymbol{g}_2, \tag{2.32}$$

the pressure in the upper fluid must become constant to ensure pressure accelerations remain finite. However, the limit value of $(1/\rho_2)\partial p_2/\partial s$ will typically be non-zero, and both viscous and pressure accelerations will be significant in the upper fluid.

The normal and shear-stress boundary conditions reduce to (Brøns *et al.* 2014; Lundgren & Koumoutsakos 1999)

$$p_1 = p_2 + T\kappa - 2\mu_1\left(\frac{\partial}{\partial s}(\boldsymbol{u}\cdot\hat{\boldsymbol{t}}) + \kappa(\boldsymbol{u}\cdot\hat{\boldsymbol{n}})\right), \tag{2.33}$$

$$\omega_1 = 2\kappa(\boldsymbol{u}\cdot\hat{\boldsymbol{t}}) - 2\frac{\partial}{\partial s}(\boldsymbol{u}\cdot\hat{\boldsymbol{n}}), \tag{2.34}$$

which are the standard free-surface boundary conditions. The vorticity and pressure in the lower fluid are independent of motion in the upper fluid, since the upper fluid cannot exert any stress on the lower fluid. For real water–air interfaces, the upper surface may still exert a shear stress on the lower fluid if velocity gradients in the upper fluid are sufficiently large, as occurs in wind-driven waves.

The flux of vorticity into fluid 1 is fully determined by the boundary condition in (2.34). Vorticity appears spontaneously at the interface to ensure the zero shear-stress condition is satisfied, and vorticity subsequently diffuses into the fluid interior along vorticity gradients. Pressure gradients and body forces drive a relative acceleration between the upper and lower fluid, generating a net circulation on the interface. The remaining balance of vorticity not sent into fluid 1 must be diffused into fluid 2, with the flux of vorticity into the upper fluid given by

$$\sigma_2 = -\frac{\mathrm{d}\boldsymbol{u}_1}{\mathrm{d}t}\cdot\hat{\boldsymbol{t}} - \frac{\partial P_2}{\partial s} + \boldsymbol{g}_2\cdot\hat{\boldsymbol{t}}, \tag{2.35}$$

where $P_2 = \lim_{\rho_2\to 0}[(p_2 - p_{2,0})/\rho_2]$, and $p_{2,0}$ is the uniform limit value of $p_2$. Although viscous stresses in the upper fluid play no role in the interface shear-stress balance, viscous accelerations in the upper fluid are not negligible, and viscous diffusion of vorticity in the upper fluid cannot be ignored.

In many cases where the free-surface approximation is applied, we are not interested in the behaviour of flow above the interface. Lundgren & Koumoutsakos (1999) treat the free surface as the interface between a viscous fluid, and an inviscid potential flow with zero density. Their formulation may be obtained from (2.22) by using a potential flow in the upper fluid,

$$\begin{aligned}\frac{\mathrm{d}\Gamma}{\mathrm{d}t} = {} & \int_{C_1} \nu\hat{\hat{\boldsymbol{n}}}\cdot\nabla\omega\,\mathrm{d}s + \int_{C_1}\hat{\hat{\boldsymbol{n}}}\cdot(\boldsymbol{v}^b - \boldsymbol{u}_1)\omega\,\mathrm{d}s + \left.\frac{p_1}{\rho_1}\right|_b - \left.\frac{p_1}{\rho_1}\right|_a + \Phi_{g,1}|_b - \Phi_{g,1}|_a \\ & + \left.\frac{\partial\Phi_2}{\partial t}\right|_b - \left.\frac{\partial\Phi_2}{\partial t}\right|_a + \gamma\boldsymbol{v}^b\cdot\hat{\boldsymbol{t}}|_b - \gamma\boldsymbol{v}^b\cdot\hat{\boldsymbol{t}}|_a + \left.\frac{1}{2}\boldsymbol{u}_1\cdot\boldsymbol{u}_1\right|_b - \left.\frac{1}{2}\boldsymbol{u}_1\cdot\boldsymbol{u}_1\right|_a.\end{aligned} \tag{2.36}$$

A net circulation may only be generated by an inviscid relative acceleration between the upper and lower fluids. Viscous stresses may transfer circulation between the interface vortex sheet and the lower fluid, to maintain the stress-free condition at the free surface. Under Lundgren & Koumoutsakos' description, no vorticity is diffused into the upper fluid. Lundgren & Koumoutsakos' result is similar to Wu's (1995) high-Reynolds-number approximation to the boundary layer of a viscous interface, suggesting that the interface vortex sheet can be interpreted as the circulation that would be found in the 'air' boundary layer above the free surface.

One difficulty in applying equation (2.36) lies in computing the potential flow above the interface. At a true free surface, one does not consider a second fluid above the interface, but that the free surface represents the boundary of a single fluid domain.

Rood (1994*b*) argues that at such boundaries, there is no need for vorticity to be conserved – vorticity may spontaneously 'appear' or 'disappear' at the free surface to satisfy the stress-free condition. However, by including the 'interface circulation', $-\int_a^b \boldsymbol{u}\cdot\hat{\boldsymbol{t}}\,\mathrm{d}s$, in the total circulation balance, Brøns *et al.* (2014) provide a description of the conservation of total circulation at stationary free surfaces.

The integral conservation law for a single fluid domain partially bounded by a free surface may be written as

$$\frac{\mathrm{d}}{\mathrm{d}t}\int_{A_1}\omega_1\,\mathrm{d}A=\int_{C_1}\nu\hat{\boldsymbol{n}}\cdot\nabla\omega\,\mathrm{d}s+\int_{C_1}\hat{\boldsymbol{n}}\cdot(\boldsymbol{v}^b-\boldsymbol{u}_1)\omega_1\,\mathrm{d}s+\int_a^b\sigma_1\,\mathrm{d}s, \tag{2.37}$$

where $a-b$ is the segment of the control-volume boundary along the free surface. Relating the vorticity flux to the tangential force balance (2.18*a*), this becomes

$$\begin{aligned}\frac{\mathrm{d}}{\mathrm{d}t}\int_{A_1}\omega_1\,\mathrm{d}A\;=\;&\int_{C_1}\nu\hat{\boldsymbol{n}}\cdot\nabla\omega\,\mathrm{d}s+\int_{C_1}\hat{\boldsymbol{n}}\cdot(\boldsymbol{v}^b-\boldsymbol{u}_1)\omega_1\,\mathrm{d}s+\int_a^b\frac{\mathrm{d}\boldsymbol{u}_1}{\mathrm{d}t}\cdot\hat{\boldsymbol{t}}\,\mathrm{d}s\\&+\left.\frac{p_1}{\rho_1}\right|_b-\left.\frac{p_1}{\rho_1}\right|_a+\Phi_{g,1}|_b-\Phi_{g,1}|_a.\end{aligned} \tag{2.38}$$

Finally, by substituting (2.13), we have

$$\begin{aligned}&\frac{\mathrm{d}}{\mathrm{d}t}\left(\int_{A_1}\omega\,\mathrm{d}A-\int_a^b\boldsymbol{u}_1\cdot\mathrm{d}\boldsymbol{s}\right)\\&\quad=\int_{C_1}\nu\hat{\boldsymbol{n}}\cdot\nabla\omega\,\mathrm{d}s+\int_{C_1}\hat{\boldsymbol{n}}\cdot(\boldsymbol{v}^b-\boldsymbol{u}_1)\omega_1\,\mathrm{d}s+\left.\frac{p_1}{\rho_1}\right|_b-\left.\frac{p_1}{\rho_1}\right|_a\\&\qquad+\Phi_{g,1}|_b-\Phi_{g,1}|_a+\frac{1}{2}\boldsymbol{u}_1\cdot\boldsymbol{u}_1|_b-\frac{1}{2}\boldsymbol{u}_1\cdot\boldsymbol{u}_1|_a-\boldsymbol{u}_1\cdot\boldsymbol{v}^b|_b+\boldsymbol{u}_1\cdot\boldsymbol{v}^b|_a.\end{aligned} \tag{2.39}$$

Here, we allow the integral $-\int_a^b\boldsymbol{u}_1\cdot\mathrm{d}\boldsymbol{s}$ to be treated as a storage of 'interface circulation'. This can be understood as the circulation contained between surface fluid and a nominally zero velocity in the empty region above the free surface. Taking this approach, interface circulation is generated by the inviscid acceleration of fluid elements on the free surface due to pressure gradients and body forces. Tangential viscous acceleration of the boundary fluid, associated with a boundary vorticity flux, transfers circulation between the interface and the fluid to maintain the shear-stress balance, but does not generate a net circulation. When the interface circulation is included in this manner, total circulation in the system is conserved, given appropriate far-field boundary conditions. Circulation may be transferred between the interface vortex sheet and the fluid interior, but the total circulation remains constant.

Note that this approach does not fundamentally disagree with that of Rood (1994*b*), who argues against the principle of 'vorticity conservation'. Rood argues against the misconception that conservation of vorticity is related to the conservation of angular momentum – vorticity is not angular momentum, so conservation of angular momentum has no bearing on the conservation of vorticity. Rood finds that vorticity may simply appear or disappear at the free surface. We adopt an alternative approach here, where the surface velocity integral is included in the total circulation, noting that the conservation law this affords may prove useful in analysing and understanding the behaviour of vorticity in various free-surface flows.

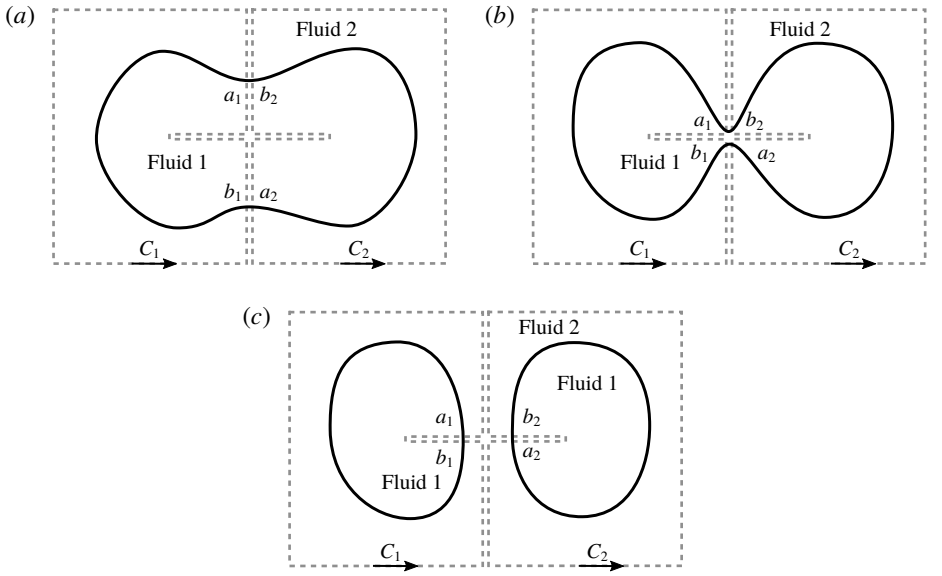


FIGURE 5. Suggested control volumes for a splitting bubble. The circulation balance for $C_1 \cup C_2$ can be expressed in terms of quantities defined on the outer boundary only, as all internal fluxes cancel on interior boundaries.

### 2.5. *Changes to the interface topology*

The analysis provided in this section is valid for a control volume spanning a single, continuous stretch of interface, topologically equivalent to figure 4. It is not immediately clear that all conclusions drawn apply to flows featuring more complex topology, such as a triple-contact point, or flows featuring topology changes, such as drop formation or wave breaking.

Equation (2.22) describes the circulation balance in terms of quantities defined only on the outer control-volume boundary. A combination of such control volumes features a 'telescoping' property, where contributions from internal boundaries cancel, and the balance of circulation for the whole system of control volumes includes contributions only from the outer boundaries. Therefore, if the flow can be covered by smaller control volumes, topologically equivalent to figure 4, the theory developed in this section may be applied. Figure 5 illustrates such a system of control volumes for the case of a splitting bubble. Although the global control volume ($C_1 \cup C_2$) does not resemble figure 4, and the interface topology changes as the flow develops, each sub-volume remains equivalent to figure 4. We anticipate that most systems can be described by a similar arrangement of control volumes, so that our formulation remains sufficiently general.

### 2.6. *Summary of theoretical findings*

Based on the preceding analysis and discussion, and from previous descriptions of interfacial vorticity dynamics, we present the following summary of the generation, transport and conservation of vorticity in two-dimensional interfacial flows. For a given control volume, which may contain an interface between two fluids, a boundary with a solid body, or a free surface,

(i) The total circulation within the control volume varies due to generation of circulation on the interface, and due to the flow of circulation through the control-volume boundary. Circulation leaves the control-volume boundary by viscous diffusion and advection in the fluid interior, and by the transport of circulation along the interface.

(ii) Circulation is generated on the interface by an inviscid relative acceleration between fluid elements on each side of the interface. This acceleration may be due to pressure gradients or body forces. There is no other mechanism by which vorticity may be generated in two-dimensional, incompressible flows.

(iii) If the tangential velocity is not continuous across the interface, circulation is contained in the interface vortex sheet. Viscous forces are responsible for the transfer of circulation between the interface vortex sheet and the fluid interior, via the boundary vorticity flux, but do not generate a net circulation in the system.

(iv) If the no-slip condition applies on the interface, no circulation is stored in the interface vortex sheet. All vorticity generated via the inviscid mechanism is sent into the fluid interior by viscous forces which enforce the no-slip condition.

(v) On no-slip viscous interfaces, the shear-stress balance governs how vorticity generated on the interface is distributed into each fluid. This condition is also responsible for driving the transfer of circulation across the interface.

(vi) At a free surface, the zero shear-stress condition mandates that the surface vorticity must be equivalent to solid-body rotation of fluid elements on the boundary. Vorticity is exchanged between the boundary fluid and the interface circulation to maintain this condition.

(vii) If there is no global pressure gradient across the interface, total circulation within the flow is conserved. Local generation of vorticity along a portion of the interface is balanced by generation of an equal quantity of opposite-sign vorticity elsewhere.

## 3. Example flows

In this section, several example flows are considered, demonstrating the insights into flow behaviour afforded by the theoretical developments outlined in the previous section. First, the role of the shear-stress balance on the generation and transport of vorticity is demonstrated by considering flows featuring stationary flat and axisymmetric interfaces. Then, the generation and conservation of vorticity at deforming interfaces is considered in the analysis of periodic travelling waves and vortex–interface interactions.

Transient solutions for the one-dimensional flow problems were obtained using an orthogonal decomposition technique, described in Özışık (1968) and based on the method of Bulavin & Kashcheev (1965). Examples featuring deformable interfaces and free surfaces were solved numerically, using a finite-difference method. A projection method due to Brown, Cortez & Minion (2001) was used, which allows second-order accuracy at solid boundaries. Boundary conditions for Brown's algorithm were adapted to suit free-surface and viscous interface flows. A boundary-fitted grid was used, to enable direct measurement of the boundary vorticity flux. Interface tracking and mesh motion is achieved through use of an ALE method (Donea *et al.* 2004). The normal velocity of nodes on the interface is determined by requiring these nodes track the interface. The tangential velocity of boundary nodes is adjusted to ensure adequate grid spacing. Nodes in the fluid interior are free to move, independently of the fluid.

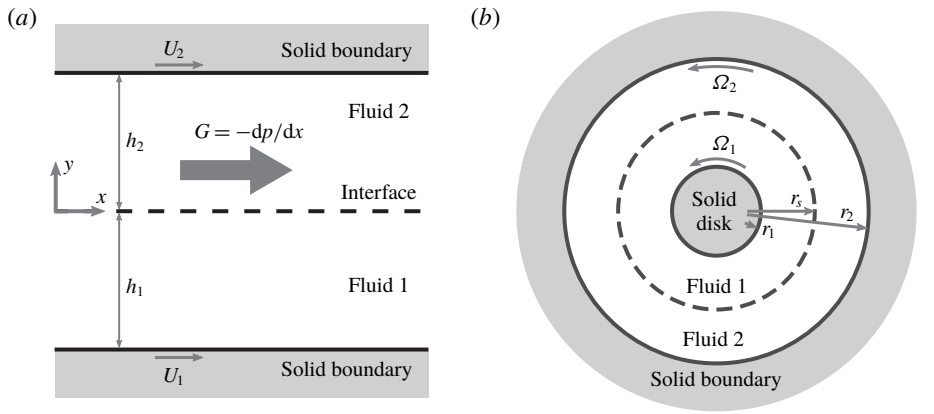


FIGURE 6. Geometry for (*a*) planar and (*b*) axisymmetric two-fluid flows. Flow in the planar channel may be driven by motion of the upper and lower solid boundaries, or by a streamwise pressure gradient. Flow in the axisymmetric arrangement is driven by rotation of the inner or outer solid disks.

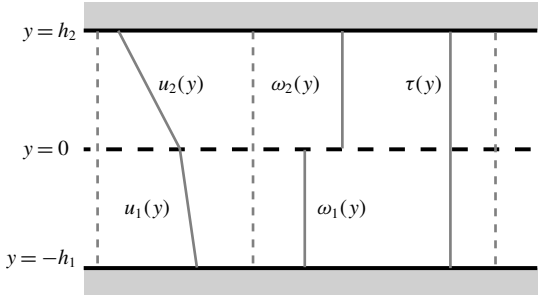


$$u_i(y) = \frac{A}{\mu_i}(y \pm h_i) + U_i \qquad (3.1a)$$

$$\omega_i(y) = -A/\mu_i \qquad (3.1b)$$

$$\tau(y) = A \qquad (3.1c)$$

$$A = \frac{U_2 - U_1}{h_1/\mu_1 + h_2/\mu_2}$$

FIGURE 7. Schematic diagram illustrating the important features of two-fluid plane Couette flow. The steady-state vorticity profile is uniform in both fluids, and the jump in vorticity across the interface satisfies the shear-stress balance. This corresponds to a linear velocity profile in both fluids, and a uniform shear stress throughout the flow.

Once the boundary nodes have been updated, internal mesh points are updated using the modified interpolated control function (MICF) approach (Hansen, Douglass & Zardecki 2005). Here, the position of internal nodes is governed by solution of an elliptic partial differential equation. The control functions that were used generate grid lines which are orthogonal to the boundaries. Elements are concentrated near the interface, and cell growth rates were set to zero on the boundary, to ensure accurate resolution of the boundary vorticity flux.

It should be noted that this finite-difference scheme obtains solutions in terms of the primitive variables, and that our formulation of vorticity dynamics is not enforced directly, but arises naturally as part of the solution. While the global conservation of circulation is often guaranteed by the boundary conditions, accurate resolution of flow near the boundary was necessary to ensure the source terms in (2.24) were balanced. This then raises the question of whether numerical schemes which automatically satisfy conservation laws such as (2.24) can be constructed, and if there is any benefit in doing so. Conservation of circulation is a natural consequence of Lundgren

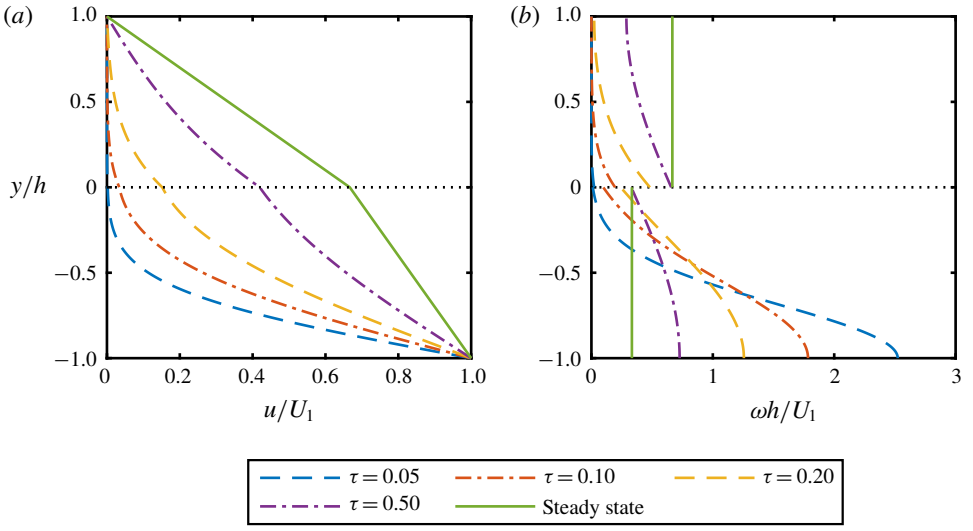


FIGURE 8. Dimensionless (*a*) velocity and (*b*) vorticity profiles at a range of time steps for transient two-fluid Couette flow. Initially stationary flow is driven by an impulsive acceleration of the lower boundary. For this example, $h_1/h_2 = 1$, $\nu_1/\nu_2 = 1$, $\mu_1/\mu_2 = 2$ and $U_2 = 0$. $\tau = t/(\bar{h}^2/\bar{\nu})$ is the dimensionless time, where overbars indicate mean values across both fluids.

& Koumoutsakos' (1999) vorticity-based scheme for free-surface flows, for example, and the theory outlined in the present article may prove useful in developing a similar scheme applicable to other kinds of interfaces. Such considerations are outside the scope of this article.

### 3.1. *Flat interface*

Two-fluid Poiseuille–Couette flow is investigated in this section, illustrating the role of the shear-stress balance on the transport of vorticity across stationary, flat interfaces. This flow configuration provides the simplest description of the shear-stress balance, as the rotational vorticity is equal to zero. Two fluid regions are separated by a flat interface, and bounded by solid boundaries, as depicted in figure 6(*a*). Couette flow is driven by a velocity difference between the upper and lower solid boundaries, while Poiseuille flow is driven by a pressure gradient along the interface. In general, flow may be a linear combination of these two basic configurations.

#### 3.1.1. *Couette flow*

Plane Couette flow occurs when there is no pressure gradient driving the flow. In this configuration, no vorticity generation occurs on the interface, and all vorticity in the flow has its origins on the upper or lower solid boundaries. The steady-state solution to the velocity, vorticity and shear-stress distributions are given by (3.1), and the general features of these distributions are illustrated in figure 7. The steady-state behaviour can be understood quite simply in terms of the total circulation and the shear-stress balance. The total circulation per unit length in the fluid is determined by

the difference in velocity between the solid boundaries,

$$\int_{-h_1}^{h_2} \omega \, \mathrm{d}y = U_1 - U_2. \tag{3.2}$$

Gradients in shear stress result in the diffusion of vorticity throughout the flow, until the vorticity profile is uniform in each fluid. Since the interface is flat, the shear-stress balance (2.27) reduces to

$$\frac{\omega_2}{\omega_1} = \frac{\mu_1}{\mu_2}, \tag{3.3}$$

and is maintained by the transport of vorticity across the interface throughout the transient flow development. The uniform steady-state vorticity in each fluid must satisfy equation (3.3).

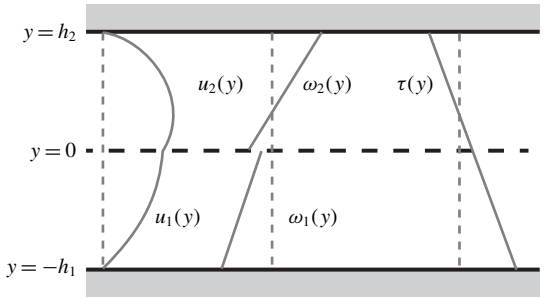


$$u_i(y) = \frac{G}{\mu_i}[Ay - y^2/2] + U_0 \tag{3.4a}$$

$$\omega_i(y) = \frac{G}{\mu_i}[y - A] \tag{3.4b}$$

$$\tau_i(y) = G[A - y] \tag{3.4c}$$

$$A = \frac{1}{2}\frac{\mu_1(h_2/h_1) - \mu_2(h_1/h_2)}{\mu_1/h_1 + \mu_2/h_2}$$

$$U_0 = \frac{G}{2}\frac{h_2 + h_1}{\mu_1/h_1 + \mu_2/h_2}$$

FIGURE 9. Schematic diagram illustrating the important features of two-fluid Poiseuille flow. The steady-state vorticity profile is linear in each fluid, with parabolic velocity profiles. The shear-stress distribution is linear, but continuous across the interface.

External acceleration of the upper/lower solid boundaries results in the generation of vorticity on the boundary, and a change in the total circulation. The generated vorticity diffuses away from the boundary and spreads throughout the flow until a new steady-state profile is reached. This process is illustrated in figure 8, which presents transient velocity and vorticity profiles for a two-fluid Couette flow driven from rest by an impulsive acceleration of the lower boundary. An animation of the velocity and vorticity profiles is also provided in the supplementary material (movie 1) available at https://doi.org/10.1017/jfm.2020.128. Vorticity generated on the lower boundary diffuses across the interface, seemingly against the vorticity gradient on the interface. While diffusion across the interface and into the region with higher surface vorticity may be counter-intuitive, it should be remembered that one may only describe the diffusion of vorticity along vorticity gradients within a single fluid domain. The transfer of circulation across an interface is governed by the viscous acceleration of boundary fluid elements, which adjusts the velocity gradients (vorticity) on each side of the interface, so that the shear-stress balance is maintained. There is no reason this process cannot be directed into the fluid with higher boundary vorticity.

### 3.1.2. *Poiseuille flow*

Two-fluid Poiseuille flow occurs when flow is driven by a pressure gradient $G = -\partial p/\partial x$, while the upper and lower walls are held stationary, $U_1 = U_2 = 0$. Vorticity is

continuously generated on the upper and lower solid boundaries, and at the interface, by inviscid relative accelerations due to pressure gradients. The vorticity fluxes on the upper and lower solid boundaries are given by

$$\sigma_{b,1} = \frac{1}{\rho_1}\frac{\partial p}{\partial x}, \tag{3.5a}$$

$$\sigma_{b,2} = -\frac{1}{\rho_2}\frac{\partial p}{\partial x}, \tag{3.5b}$$

while the rate of vorticity creation at the interface is

$$\sigma_{i,1} + \sigma_{i,2} = \left(\frac{1}{\rho_2} - \frac{1}{\rho_1}\right)\frac{\partial p}{\partial x}. \tag{3.6}$$

The net rate of vorticity creation across both solid boundaries and the interface is zero,

$$\sigma_{b,1} + \sigma_{b,2} + \sigma_{i,1} + \sigma_{i,2} = 0, \tag{3.7}$$

so that the total amount of circulation in the system remains constant, and is equal to zero.

The general features of steady-state Poiseuille flow are illustrated in figure 9, with analytic solutions to the velocity, vorticity and shear-stress profiles given by (3.4). The vorticity profile in each fluid is linear, indicating a constant rate of diffusion in each fluid. Vorticity is continually generated on the solid boundaries and diffuses into the fluid interior. The vorticity flux out of each side of the interface is equal and opposite to the vorticity flux on the corresponding solid boundary, maintaining the steady-state equilibrium.

While the vorticity generation rate determines the net vorticity flux out of the interface, the vorticity flux into each fluid must ensure the shear-stress balance is maintained on the interface. Consider transient development of two-fluid Poiseuille flow in an initially stationary fluid, depicted in figure 10, and for which a transient animation is provided in movie 2 (supplementary material). Initially, most vorticity remains in boundary layers of thickness $\sqrt{\nu t}$, and vorticity generated on the solid boundaries has a negligible effect on the interface shear-stress balance. The ratio of initial vorticity fluxes into each fluid from the interface is equal to

$$\frac{\sigma_{1,i}}{\sigma_{2,i}} = \frac{\mu_2}{\mu_1}\sqrt{\frac{\nu_1}{\nu_2}}, \tag{3.8}$$

and depends on the ratio of boundary vorticity required to satisfy the shear-stress balance, and the rate at which vorticity diffuses away from the interface. For the example in figure 10 the higher rate of diffusion in the lower fluid is balanced by the requirement of a higher surface vorticity in the upper fluid, and the initial vorticity fluxes on both sides of the interface are equal.

As flow develops, the ratio of interface vorticity fluxes is affected by vorticity generated on the solid boundaries. For the example in figure 10, negative vorticity generated on the lower boundary acts to reduce the interface boundary vorticity in fluid 1, while positive vorticity generated on the upper boundary reinforces the interface vorticity in fluid 2. To maintain the shear-stress balance, a larger proportion of the positive vorticity generated on the interface is diffused into the lower fluid. The flux of vorticity into fluid 2 decreases, eventually becoming negative. This process continues until a steady state is approached, where the solid boundary fluxes are balanced by the interface vorticity fluxes in each fluid. Note that the net vorticity flux on the interface does not change, only the distribution of fluxes into each fluid.

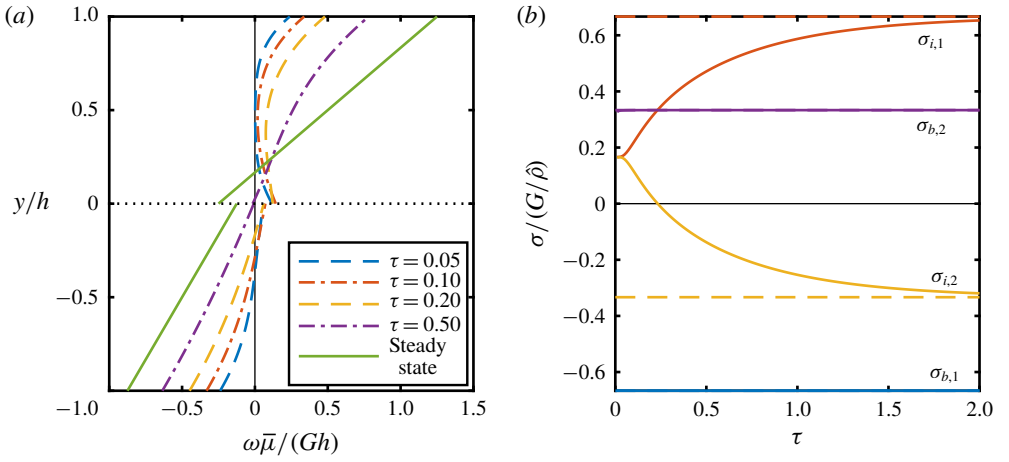


FIGURE 10. (*a*) Transient vorticity profiles and (*b*) time history of the interface and boundary vorticity fluxes for two-fluid Poiseuille flow with $h_1/h_2 = 1$, $\mu_1/\mu_2 = 2$, $\nu_1/\nu_2 = 4$, and $Gh^3/(\bar{\mu}\bar{\nu}) = 10$. $\tau = t/(\bar{h}^2/\bar{\nu})$ is the dimensionless time, while overbars indicate the mean values across both fluids. $\hat{\rho} = \bar{\mu}/\bar{\nu}$ is the mean density. Dashed lines in (*b*) indicate the steady-state asymptotes.

### 3.2. *Axisymmetric interface*

In the planar interface flows considered thus far, the rotational vorticity is zero, greatly simplifying the shear-stress balance. The influence of rotational vorticity on the shear-stress balance is highlighted in the analysis of two-fluid Taylor–Couette flow, which is described by the geometry in figure 6(*b*). As with plane Couette flow, vorticity is generated by acceleration of the inner or outer solid boundaries. Total circulation across both fluids is determined by the boundary velocities, taking the circumference of each boundary into account,

$$\int_A \omega \, \mathrm{d}A = 2\pi(\Omega_2 r_2^2 - \Omega_1 r_1^2). \tag{3.9}$$

Gradients in viscous stresses diffuse vorticity throughout the flow, producing a uniform steady-state vorticity profile in each fluid.

The main difference between axisymmetric and plane Couette flow is the influence of rotational vorticity on the interface shear-stress balance. The distribution of vorticity on each side of the interface must satisfy equation (2.27), which reduces to

$$\frac{\mu_1}{\mu_2} = \frac{\omega_2 - 2u_{\theta,s}/r_s}{\omega_1 - 2u_{\theta,s}/r_s}, \tag{3.10}$$

where $u_{\theta,s}$ is the azimuthal velocity on the interface, and $\omega_r = 2u_{\theta,s}/r_s$ is the rotational vorticity. Although the shearing vorticity, $\omega_{\tau,i} = \omega_i - \omega_r$, must be of the same sign in each fluid, the total vorticity need not.

This is demonstrated by the transient vorticity profiles presented in figure 11, for which an animation is provided in movie 3. Negative (clockwise-oriented) vorticity is generated by impulsive acceleration of the inner disk, radially beneath an interface with a viscosity ratio of $\mu_1/\mu_2 = 5$. As this negative vorticity begins to diffuse across

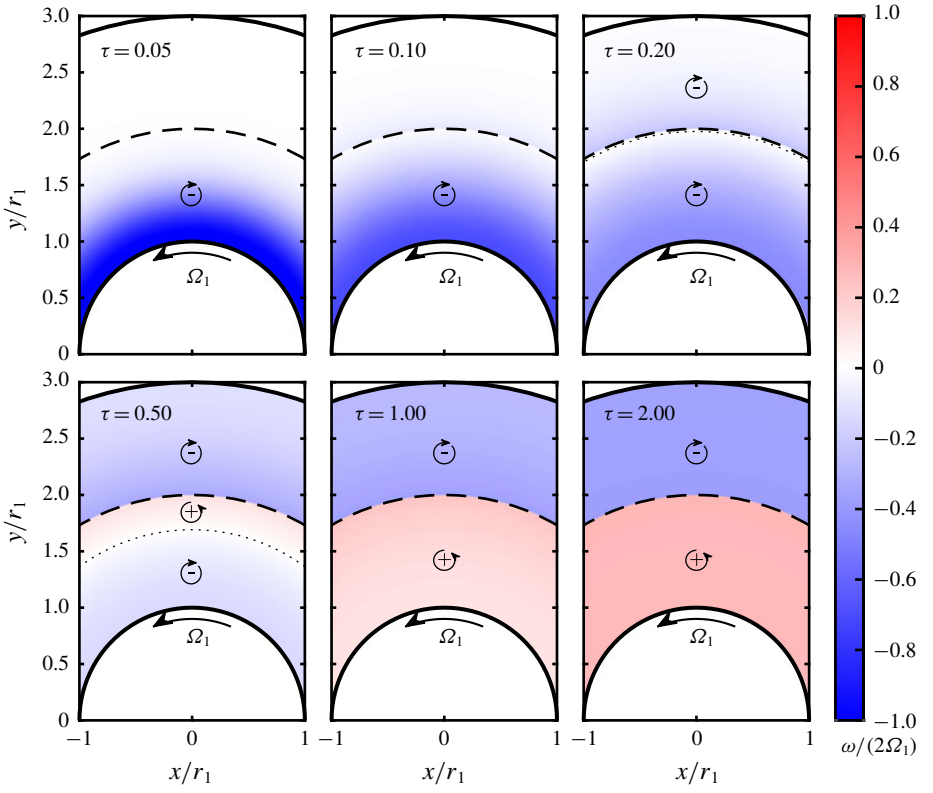


FIGURE 11. Normalised vorticity contour plots at several instants for two-fluid Taylor–Couette flow, with $r_2/r_1 = 3$, $r_s/r_1 = 2$, $\mu_1/\mu_2 = 5$, $\nu_1/\nu_2 = 1$ and $\Omega_2 = 0$. $\tau = t/(\hat{r}^2/\bar{\nu})$ is the dimensionless time, where $\hat{r} = (r_2 - r_1)/2$ and $\bar{\nu} = (\nu_1 + \nu_2)/2$.

the interface, positive vorticity appears on side 1 of the interface, and begins to diffuse into the lower fluid. Negative vorticity continues to diffuse out of the interface into fluid 2, balanced by an equal flux of positive vorticity into fluid 1. In the steady state, fluid 1 is a region of uniform positive vorticity, while fluid 2 has a uniform distribution of negative vorticity.

Appearance of positive vorticity in fluid 1 can be explained by the shear-stress balance (3.10). Figure 12(*a*) presents the vorticity on each side of the interface, along with the decomposition into rotation and shearing components. Diffusion of negative vorticity across the interface is associated with an acceleration of the interface, producing a positive rotational vorticity on the interface. Due to the reasonably high viscosity ratio, the (negative) shearing vorticity in fluid 2 must be much larger than the shearing vorticity in fluid 1. The required negative shearing vorticity in fluid 1 is smaller than the positive rotational vorticity, so the surface vorticity in fluid 1 must be positive.

The total circulation balance for this flow is presented in figure 12(*b*). There is no pressure gradient or body force along the interface, so no net circulation is generated on the interface. The flux of positive vorticity out of the interface into fluid 1 is balanced by an equal flux of negative circulation into the upper fluid, and the total circulation remains constant. If the circulation contained in the inner solid disk is included in the total circulation balance, then circulation is also conserved during the

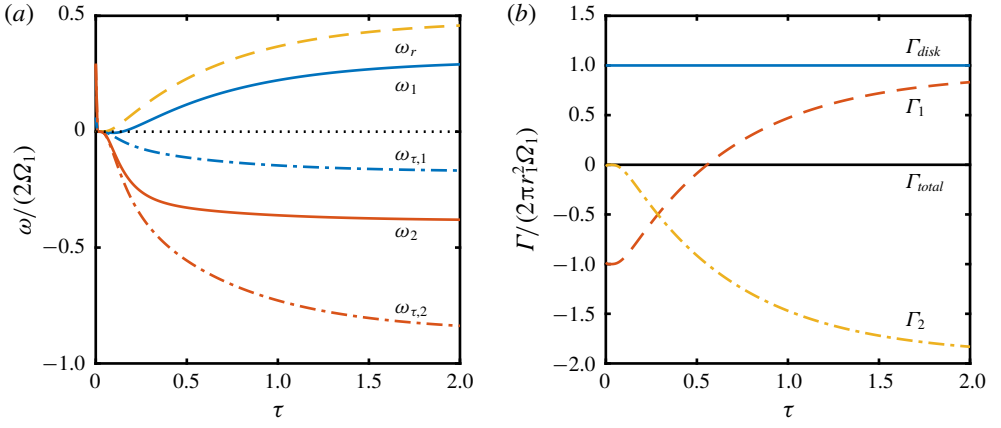


FIGURE 12. Time histories of the (*a*) normalised interface boundary vorticity, including decomposition into shear and rotation components, and (*b*) total circulation balance, for the flow displayed in figure 11.

initial generation of vorticity on the solid boundary (Brøns *et al.* 2014). The quantity of negative circulation diffused into the fluid is balanced by the appearance of an equal quantity of positive circulation in the solid disk.

The example considered in this section bears much similarity to the flow induced by a rotating cylinder beneath an axisymmetric stress-free boundary, studied by Brøns *et al.* (2014), and illustrated in their figure 10. Negative vorticity generated on the solid disk 'disappears' into the free surface, accompanied by acceleration of the free-surface fluid. Positive vorticity appears on the boundary to satisfy the stress-free condition, and diffuses into the fluid. When the solid disk and interface circulation are included in the total circulation balance, total circulation is conserved throughout the initial acceleration of the solid boundary and subsequent interaction of vorticity with the free surface. The loss of negative vorticity, and appearance of positive vorticity, on the free surface is balanced by the appearance of negative circulation in the interface. The similarities in the circulation balance for Brøns *et al.*'s free-surface flow, and the present two-fluid case, support the interpretation of 'interface circulation' as circulation that would be found on the 'air' side of a free-surface flow.

### 3.3. *Periodic travelling wave*

We now turn our attention to the generation and transport of vorticity across deformable interfaces. The first example considered is that of a periodic travelling wave on either a viscous interface or a free surface. As discussed previously, these flows may be analysed in a frame of reference travelling at the wave velocity, where normal velocity of the interface is negligible. Although the wave amplitude decays due to viscous dissipation, the time scale associated with this process is much longer than the wave period, leading to a quasi-steady interface in the moving frame. While the description of vorticity generation given by Brøns *et al.* (2014) correctly describes the flow when viewed from the moving reference frame, it cannot explain flow behaviour when using the stationary reference frame. An important result of the present formulation is that the description of vorticity generation and conservation it

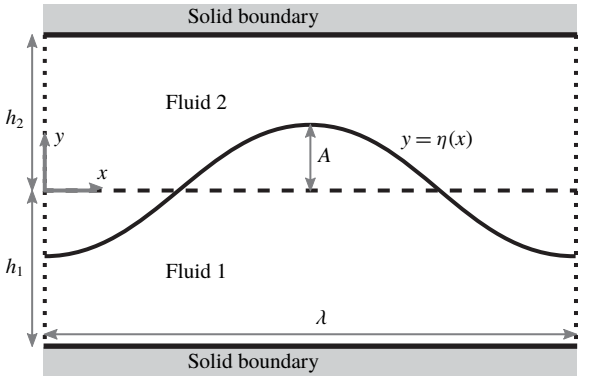


FIGURE 13. Initial problem set-up for a periodic travelling wave on the viscous interface between two fluids. The initial wave of amplitude $A$ and wavelength $\lambda$ is an irrotational, two-fluid Stokes wave. Periodic boundary conditions are enforced at the left and right boundaries. The solid boundaries are assumed to be sufficiently far from the interface that they do not significantly influence the vorticity field. For the free-surface case, the upper fluid is ignored, and the interface replaced by a free surface.

| Case | A | B | C | D |
|---|---|---|---|---|
| $\rho_1/\rho_2$ | 2 | 10 | 100 | Free surface |
| $Re = c\lambda/\nu_1$ | $5.87 \times 10^4$ | $8.12 \times 10^4$ | $1.01 \times 10^5$ | $1.02 \times 10^5$ |
| $Fr = c/\sqrt{g\lambda}$ | 0.232 | 0.321 | 0.400 | 0.404 |
| $A/\lambda$ | 0.025 | 0.025 | 0.025 | 0.025 |
| $\nu_2/\nu_1$ | 1 | 1 | 1 | 1 |
| $H_1/\lambda$ | 2.5 | 2.5 | 2.5 | 2.5 |
| $H_2/\lambda$ | 2.5 | 2.5 | 2.5 | 2.5 |

TABLE 1. Parameter space investigated for viscous travelling waves. $c$ is the wave speed, estimated using irrotational Stokes wave theory.

affords does not depend on either the frame of reference, or normal motion of the interface. The following analysis remains unchanged if the waves are viewed from the stationary reference frame, where significant normal motion of the interface occurs.

Figure 13 demonstrates the geometry for this problem, while the parameter set investigated is provided in table 1. Irrotational Stokes waves are used as the initial conditions, using Fenton's (1985) fifth-order solution for the free-surface case, and Tsuji and Nagata's (1973) fifth-order solution for interfacial waves. The primary variable considered is the density ratio, which ranges from $\rho_1/\rho_2 = 2$ to free-surface conditions. The wave steepness, gravitational strength and viscosity were held constant across all cases; these variables will affect the quantity of vorticity generated, but the general flow structure will not be significantly altered. As the wave speed, $c$, changes with density ratio, the respective Reynolds ($Re$) and Froude ($Fr$) numbers also vary with the density ratio. Because of the quasi-steady nature of this flow, results presented for $\tau = t/(\lambda/c) = 10$ represent the general flow behaviour. The effects of surface tension are not considered here.

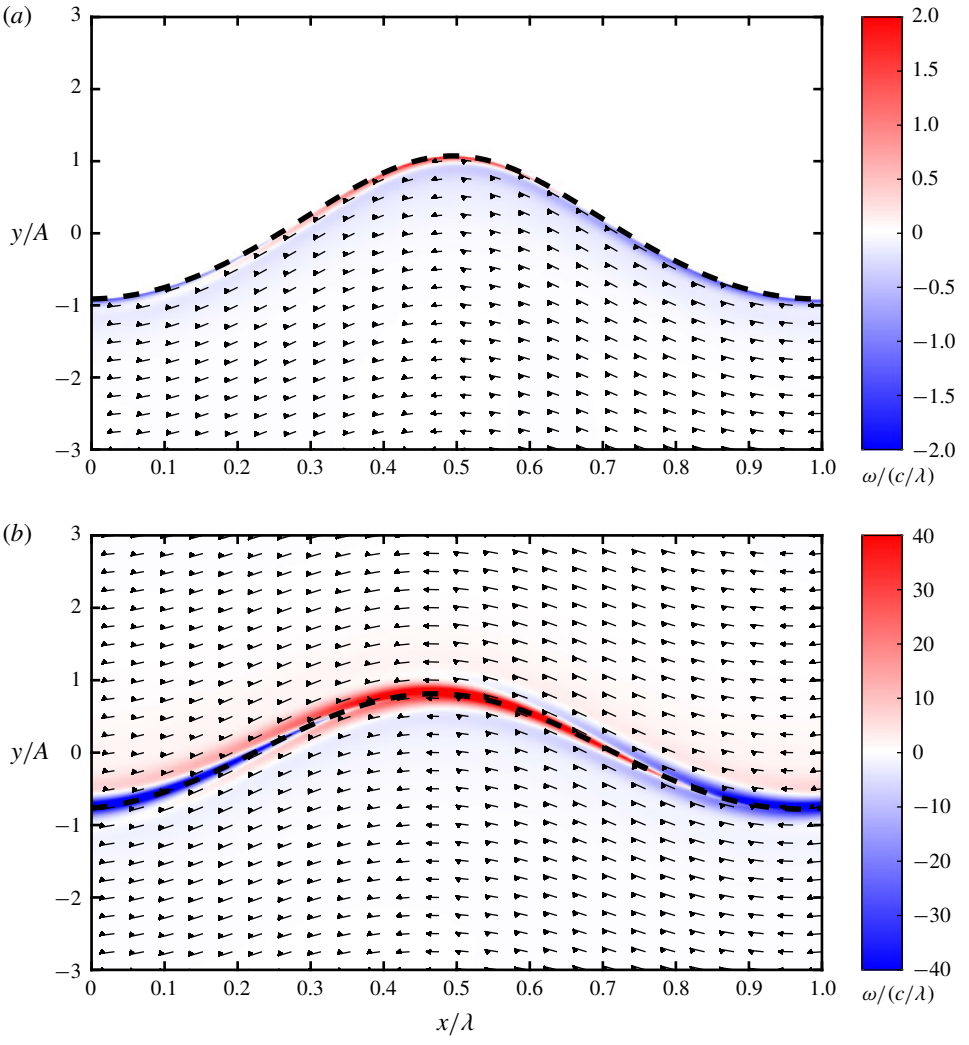


FIGURE 14. Vorticity contours and velocity vectors for periodic travelling waves along (*a*) a free surface, and (*b*) a viscous interface with $\rho_1/\rho_2 = 2$. The vertical scale is greatly exaggerated for clarity. Contours are presented at a dimensionless time $\tau = t/(\lambda/c) = 10$, where $c$ is the wave speed.

### 3.3.1. *Free-surface wave*

Vorticity contours and velocity vectors for the free-surface wave are presented in figure 14(*a*), and an animation of this flow is provided in movie 4. Longuet-Higgins (1960) discusses the formation of vorticity in the boundary layer of a free-surface wave. Most of the vorticity is located within a thin layer of alternating-sign vorticity, of thickness $O(\sqrt{\nu T})$, where $T$ is the wave period. The stress-free condition requires that boundary fluid elements rotate at a rate equivalent to solid-body rotation on the free surface, requiring positive (anti-clockwise) vorticity at the wave crest, and negative (clockwise) vorticity at the wave trough. When viewed from the moving reference frame, this rotation is due to fluid elements following the curvature of the wave; from the stationary reference frame, fluid elements rotate as the wave travels

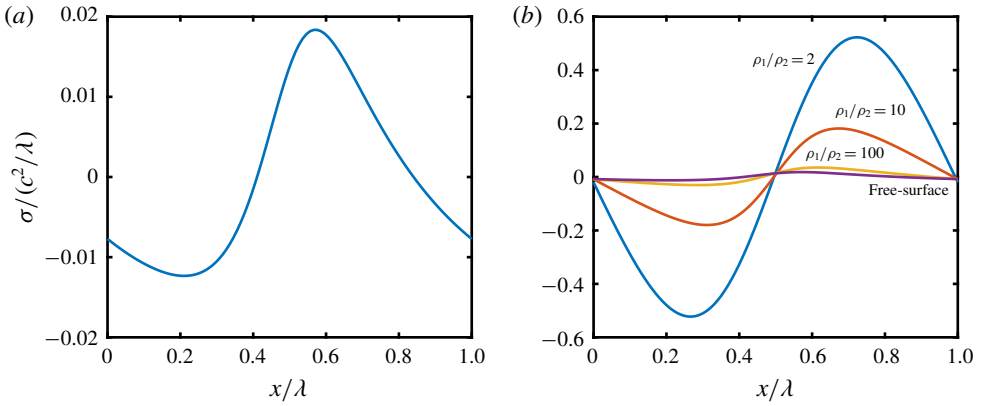


FIGURE 15. Distribution of the interface vorticity flux into the lower fluid ($\sigma_1$) along (*a*) free-surface and (*b*) viscous interface waves with a range of density ratios.

along the interface. A fluid element will encounter a flux of positive vorticity as it approaches the wave crest (or the wave crest approaches it), and a flux of negative vorticity as it approaches the wave trough, to maintain this condition. The free-surface vorticity flux profile in figure 15(*a*) reflects this behaviour. A positive vorticity flux is observed between $x/\lambda \approx 0.8$ to 0.4, as surface fluid approaches the wave crest. The vorticity flux is negative in the remaining regions, as fluid approaches the trough. It is stressed that the boundary vorticity flux beneath the free surface is due to viscous stress gradients in the fluid, and acts to ensure the condition of zero shear stress is satisfied on the free surface.

Positive vorticity from the wave crest is carried by advection to the wave trough, where it suffers cross-diffusive annihilation with the negative vorticity that appears there. Similarly, negative vorticity from the wave trough is annihilated by positive vorticity from the wave crest. The time scale associated with this process is the wave period, $T$, so cross-diffusive annihilation of vorticity occurs over a length scale of $\sqrt{\nu T}$. Due to an imbalance in the quantity of negative and positive vorticity diffused into the boundary layer, a net amount of negative circulation 'survives' this cross-annihilative process. This results in a growing layer of negative 'streaming vorticity', which is clearly visible in movie 4.

This behaviour can be also be observed in the circulation time history presented in figure 16(*a*). As flow develops, a net amount of negative circulation is diffused into the fluid. However, if the interface circulation is included in the total circulation balance, then the total circulation is conserved. Due to the periodic boundary conditions employed, no net circulation is generated in the interface. The net flux of negative circulation into the fluid is balanced by a viscous acceleration of the free-surface fluid, and the appearance of positive circulation in the interface.

### 3.3.2. *Interfacial wave*

Vorticity contours and velocity vectors for the viscous interface wave, with $\rho_2/\rho_1 = 2$, are presented in figure 14(*b*), and the corresponding animation is provided in movie 5. Local pressure gradients result in the generation of vorticity along the interface, with positive vorticity observed on both sides of the interface at the wave crest, and negative vorticity in both fluids at the wave trough. As with the

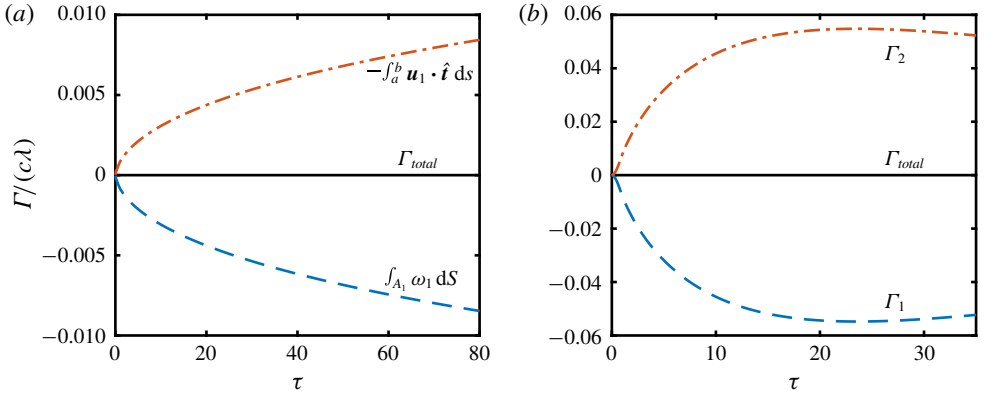


FIGURE 16. Time histories of total circulation for the (*a*) free-surface and (*b*) viscous interface waves depicted in figure 14.

free-surface wave, most of this vorticity remains within a thin boundary layer on the interface. The vorticity generated at one section of the wave suffers cross-diffusional annihilation with alternate-signed vorticity generated elsewhere as vorticity is carried by fluid elements along the interface (or, when viewed from the stationary frame, as successive wave crests/troughs travel past a particular fluid element on the interface).

Figure 16(*b*) presents the net circulation balance for the interfacial wave described in figure 14(*b*). Although local generation of vorticity by pressure gradients occurs, the periodic boundary condition ensures that the net vorticity generated is zero – positive vorticity generated along one section of the interface is balanced by an equal amount of negative circulation generated elsewhere. However, the net flux of vorticity into each fluid is not zero. A negative net circulation is diffused into the lower fluid, balanced by an equal quantity of positive circulation diffused into the upper fluid. In a manner similar to flow beneath a free-surface wave, most of the vorticity generated on the interface is eliminated by cross-diffusive annihilation within a boundary layer of thickness $O(\sqrt{\nu T})$. There is a second-order net flow of negative circulation into the interior of the lower fluid, and a net flow of positive vorticity into the upper fluid.

The second-order streaming vorticity in both free-surface and viscous interface waves can be explained by the rate at which vorticity diffuses away from the boundary. If the boundary vorticity on one side of the interface is depleted more rapidly by viscous diffusion, the flux of vorticity into that fluid must be increased to maintain the shear-stress balance. Concave geometry, such as beneath the wave crest or above the wave trough, restricts the diffusion of vorticity away from the boundary, while convex geometry allows greater diffusion of vorticity into the fluid interior. In the lower fluid, the negative vorticity flux at the wave trough will exceed the positive vorticity flux near the wave crest, sending a net negative circulation into this fluid. This argument is reversed in the upper fluid, yielding a net flux of positive vorticity.

While the net generation of vorticity on the interface is zero, local vorticity generation by pressure gradients along the interface still occurs. The interface pressure profiles presented in figure 17(*a*) indicate that the wave trough is a region of increased pressure, compared to the lower pressure in the wave crest. Although pressure gradients are approximately equal on both sides of the interface, the difference in inertia of fluid elements either side of the interface results in an inviscid relative acceleration, and the generation of circulation on the interface. The local vorticity

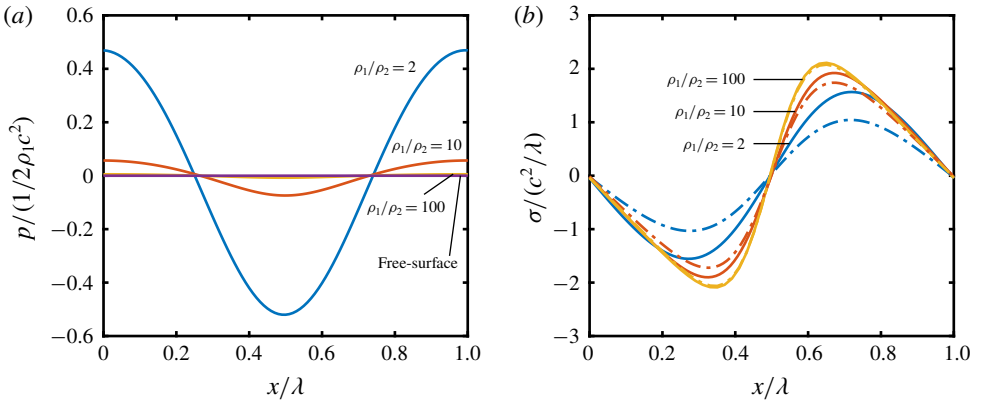


FIGURE 17. (*a*) Pressure distribution along the surface of interfacial waves with a range of density ratios. The jump in pressure across the interface is negligible. (*b*) Local vorticity generation rate along the interface. Solid lines in (*b*) indicate the net vorticity flux, $\sigma_1 + \sigma_2$, while dash-dotted lines indicate the flux into the upper fluid, $\sigma_2$.

generation rates along the interface, given in figure 17(*b*), can be explained by the interface pressure gradient. Fluid elements on the interface are accelerated by the favourable pressure gradient between $x/\lambda = 0.5$ and 1.0. This pressure gradient acts to accelerate the upper fluid at a greater rate than the lower fluid, generating anti-clockwise (positive) circulation in the interface. An equal quantity of clockwise (negative) circulation is generated by the adverse pressure gradient along the rear half of the wave. Note that viscous forces which enforce the no-slip condition prevent any actual relative acceleration between fluid elements, diffusing all circulation into the fluid interior via the associated boundary vorticity fluxes.

While pressure gradients on the interface decrease as the density ratio is increased, the rate of vorticity generation increases. The decrease in inertia of the upper fluid is more significant than the decrease in pressure gradient, producing a greater inviscid relative acceleration of fluid elements. While the net vorticity generation rate increases with the density ratio, the shear-stress balance requires that a larger proportion of this vorticity be diffused into the upper fluid. As a result, vorticity fluxes into the lower fluid decrease as the jump in density is increased. As demonstrated in figure 15(*b*), the vorticity flux into the lower fluid approaches the free-surface distribution as the density ratio is increased. The limiting distribution of $\sigma_1$ is not zero, but instead takes on the value required to maintain the stress-free condition on the free surface.

The shear-stress balance constrains how circulation generated on the interface is distributed into each fluid. Surface vorticity profiles for viscous interfaces with $\rho_1/\rho_2 = 2$ and $\rho_1/\rho_2 = 100$ are presented in figure 18, including the decomposition into shearing and rotational vorticity. For low values of the density ratio, the shearing vorticity dominates the rotational vorticity, and the shear-stress balance may be approximated as

$$\frac{\omega_2}{\omega_1} \approx \frac{\mu_2}{\mu_1} = \frac{\rho_2}{\rho_1}. \tag{3.11}$$

As the density/viscosity ratio is increased, a larger proportion of vorticity generated on the interface must be diffused into the upper fluid, and the boundary vorticity in the lower fluid decreases. Figure 19 compares the surface vorticity in the lower

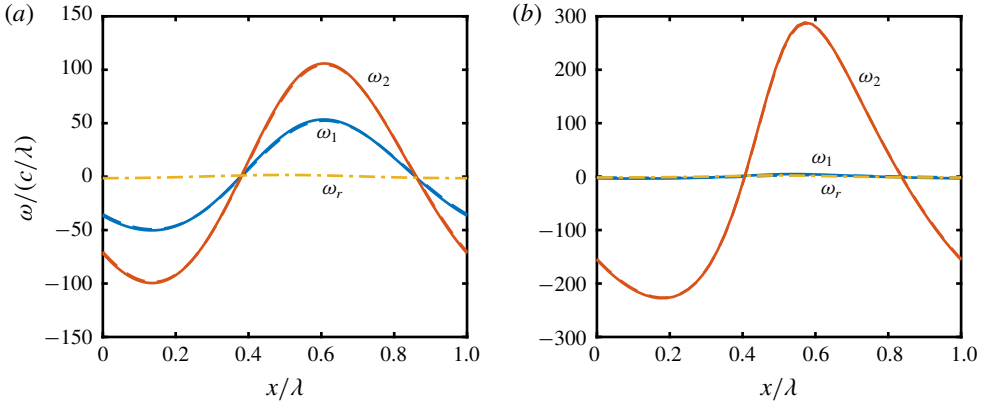


FIGURE 18. Surface vorticity profiles, including the decomposition into rotation and shearing vorticity, for viscous interface waves with (*a*) $\rho_1/\rho_2 = 2$ and (*b*) $\rho_1/\rho_2 = 100$. Solid lines represent total vorticity, while dashed lines indicate the shearing vorticity (nearly indistinguishable from the total vorticity).

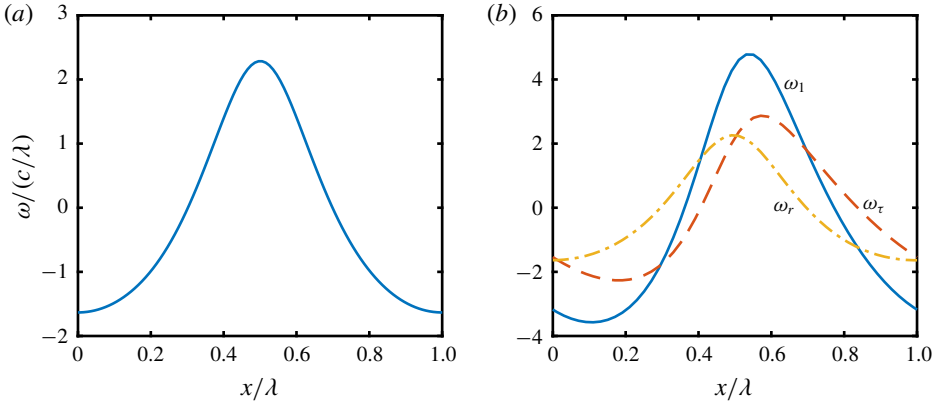


FIGURE 19. Surface vorticity in the lower fluid for periodic waves on (*a*) a free surface, and (*b*) a viscous interface with $\rho_1/\rho_2 = 100$. Rotation and shear vorticity components are provided for the viscous interface case.

fluid, for $\rho_1/\rho_2 = 100$, to the free-surface distribution. As the interface approaches the free-surface limit, the shearing vorticity in the lower fluid decreases, and the surface vorticity approaches the rotational vorticity. However, for any finite density ratio there will be a typically non-zero residual shearing vorticity, $\omega_{\tau,1} = \omega_1 - \omega_r$, which has the following approximate relationship to the vorticity in the upper fluid,

$$\omega_2 \approx \frac{\mu_1}{\mu_2}[\omega_1 - \omega_r]. \tag{3.12}$$

The results presented in this section suggest the following description of vorticity generation at high-density-ratio interfaces, such as the typical air–water interface. Under the free-surface approximation, the flux of vorticity on the lower side of the interface is determined by viscous stress gradients in the lower fluid, independent

of motion in the upper fluid. If velocity gradients in the upper fluid are sufficiently high, such as for wind-driven waves, a non-zero shearing vorticity in the lower fluid, proportional to the vorticity in the upper fluid, should also be considered. The upper fluid will suffer a greater 'inviscid' acceleration due to pressure forces than the lower fluid, generating circulation in the interface. The majority of this circulation will be diffused into the boundary layer on the air side of the interface, with only a small portion sent into the lower fluid to maintain the shear-stress balance. The similarities between the total circulation balances in figure 16 suggest that the 'interface circulation' above a free surface is indicative of the circulation that would be found on the air side of the interface.

The importance of flow structures on the air side of a water–air interface has been highlighted by Buckley & Veron (2017, 2019), who suggest that turbulent vortex structures above wind-driven water waves are responsible for increased momentum and mass transport across the ocean surface. These turbulent structures form when boundary layer vorticity, generated along the windward side of the wave, separates at the wave crest. The generation of vorticity in the boundary layer is easily understood under the present formulation, and the description is identical to the previous examples considered in this section. Moreover, the influence of these airflow structures on the vorticity field beneath the wave can be readily discussed under our description, by making use of the shear-stress balance on the interface.

### 3.4. *Vortex-pair interactions with a free surface or viscous interface*

While the viscous waves examined in § 3.3 can be analysed in a reference frame where the surface is approximately steady in time, the present description of vorticity generation does not require a stationary interface, and the same mechanisms of vorticity generation apply in flows featuring moving interfaces as for those where the interface remains stationary. The interaction of a vortex pair with a free surface or viscous interface presents a typical case of vortex–surface interactions where the interface cannot be described as stationary in any reference frame. Although normal motion of the interface occurs, under the present formulation the generation and conservation of vorticity can be described just as easily as the previous examples featuring stationary interfaces.

Here, we consider the flow configuration described by figure 20. A pair of counter-rotating vortices, of strength $k$, radius $r_m$ and separated by a distance, $a$, is initially positioned at a depth, $H$, beneath an undisturbed interface. For numerical simulations, a symmetry boundary condition is applied at the centre plane. The semi-infinite domain is made finite by the inclusion of solid upper and lower boundaries, positioned $10a$ above and below the undisturbed surface, and a stress-free right boundary, situated a distance of $10a$ from the centre plane.

Following Ohring and Lugt's (1991) investigation of the interaction of a vortex pair with a free surface, the following dimensionless parameters are sufficient to describe the flow: the Froude number, $Fr = k/\sqrt{ga^3}$, the Reynolds number, $Re = k/\nu_1$, the dimensionless vortex depth, $\delta = H/a$ and the dimensionless vortex radius, $r_m/a$. For the viscous interface problem, the interface jump ratios $\rho_1/\rho_2$ and $\nu_1/\nu_2$ are also required. All results presented here are for $Re = 100$, $\delta = 3$, $r_m/a = 0.25$, $\nu_1/\nu_2 = 1$ and $Fr = 0.2$, unless stated otherwise. The main variable considered is the density ratio, which ranges from $\rho_1/\rho_2 = 2$ to free-surface conditions. These conditions were chosen to enable comparison with the $Fr = 0.2$ flow in Ohring & Lugt (1991). Changes to $Re$, $\delta$ and $r_m/a$ all have a broadly similar effect (Ohring & Lugt 1991), which is not considered here.

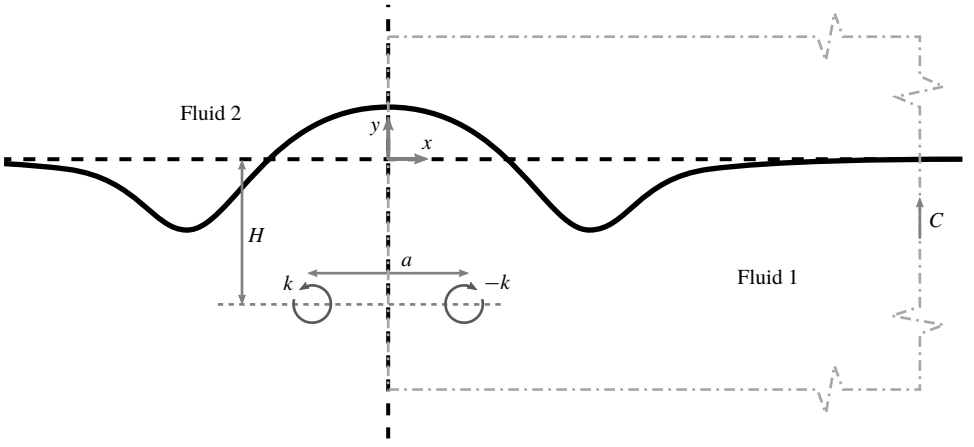


FIGURE 20. Geometry of a vortex pair beneath a viscous interface. The vertical centre line is a symmetry plane. $C$ is a circulation contour bounding the semi-infinite domain to the right-hand side of the symmetry plane.

Surface tension is not considered in any of the examples presented in this section. For the free-surface case, surface tension acts to reduce the curvature and deformation of the interface, thereby reducing the flux of vorticity out of the free surface (Ohring & Lugt 1991). For the viscous interface flows, surface tension may also affect the rate of vorticity generation through the Laplace pressure gradient, as demonstrated by (2.31).

The initial velocity field is described by a pair of Lamb vortices, each with a velocity profile

$$v_{\phi,i} = \frac{2\pi k}{r_i}[1 - \exp(-(r_i/r_m)^2)], \tag{3.13}$$

where $v_{\phi,i}$ is the azimuthal velocity about vortex $i$, and $r_i$ is the distance to the centre of each vortex. The velocity at any point is the sum of contributions from both vortices.

Vorticity contours for the free-surface flow are presented in figure 21(*a*), for a selection of flow times. Animations for both the free-surface and viscous interface flows are provided in movie 6. Ohring & Lugt (1991) have previously discussed the generation of vorticity during the interaction of a vortex pair with a free surface. In particular, note the similarity of figure 21(*a*) with Ohring and Lugt's figure 8, which are for identical Froude numbers. As the vortex approaches the surface, fluid above the centre of the vortex pair is elevated, accompanied by the appearance of a sharp depression, or 'scar', in the surrounding fluid. Circulation is transferred between the interface vortex sheet and the fluid to ensure the shear-free condition is satisfied, as determined by rotation and curvature of the interface.

The majority of vorticity generated on the boundary has positive (anti-clockwise) orientation, and is of sign opposite to that of the primary vortex. This secondary vorticity is drawn away from the free surface by the primary vortex. Ohring & Lugt (1991) find that for higher Froude number flows, sharper curvature of the interface results in a greater quantity of vorticity generated, and the appearance of a secondary vortex which orbits the primary vortex. In our simulations, overturning of the free surface was found to occur at much lower Froude numbers than reported by Ohring

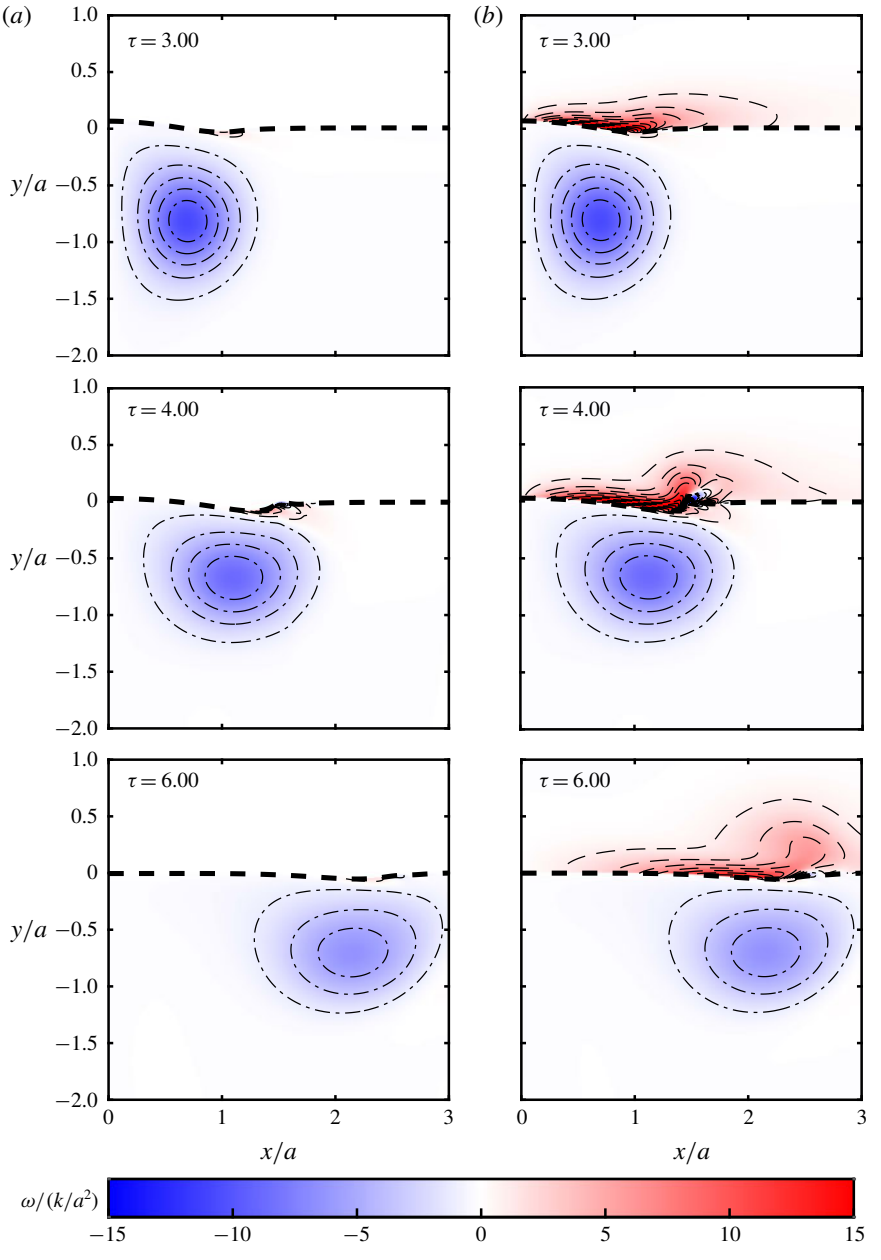


FIGURE 21. Vorticity contours depicting the interaction of the right half of a vortex pair with (*a*) a free surface, and (*b*) a viscous interface with $\rho_1/\rho_2 = 100$. $Fr = 0.2$ in both cases. $\tau = t/(a^2/k)$ is the dimensionless flow time. Non-dimensional vorticity contour levels are plotted for $\omega/(k/a^2) = \ldots, -3, -1, +1, +3, \ldots$.

and Lugt, restricting our boundary-fitted grid to low Froude numbers. A linearised small-angle approximation was used by Ohring and Lugt in their free-surface boundary conditions, which is clearly not applicable at higher Froude numbers. While we do not present flows featuring breaking of the interface in this article, the mechanisms

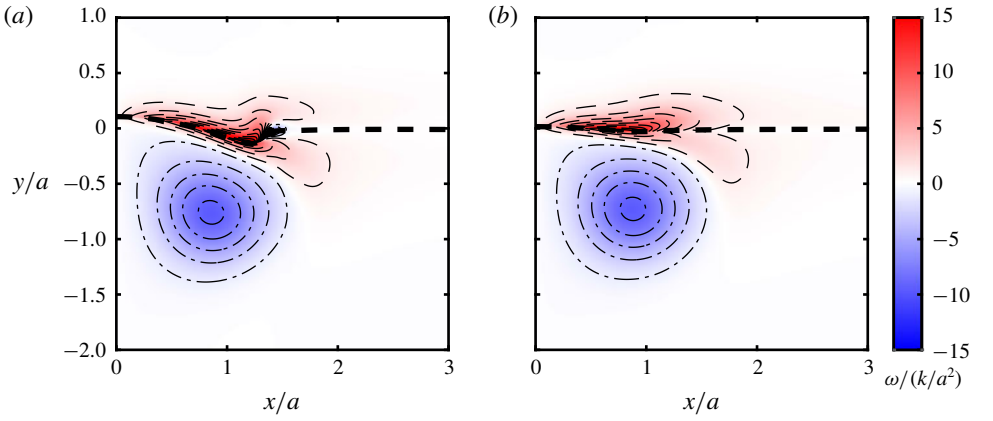


FIGURE 22. Vorticity contours for the interaction of a vortex pair with a viscous interface, with $\rho_1/\rho_2 = 2$, for (*a*) $Fr = 0.2$ and (*b*) $Fr = 0.1$, at $\tau = 3.5$. Note the similarity in the vorticity field, despite the stark differences in interface curvature. Non-dimensional vorticity contour levels are plotted for $\omega/(k/a^2) = \ldots, -3, -1, +1, +3, \ldots$.

of vorticity generation, and the principle of vorticity conservation, presented here still apply to such flows.

Vorticity contours for the viscous interface interaction, with a density ratio of $\rho_1/\rho_2 = 100$, are presented in figure 21(*b*). The shape of the interface, and the vorticity field below the interface, are nearly identical to the free-surface case. The free-surface flow is thus a suitable approximation to the flow beneath an interface with large density and dynamic viscosity ratios. The low viscosity in the upper fluid ensures that the shearing vorticity in the lower fluid is small. Rotational vorticity dominates the shear-stress balance in the lower fluid and the flux of vorticity into this fluid ensures boundary fluid elements rotate at a rate equivalent to solid-body rotation.

Circulation is generated along the interface by inviscid relative accelerations caused by pressure gradients along the interface. This relative acceleration occurs in the same manner as discussed for interfacial waves, and can be inferred directly from the vorticity contours in figure 21(*b*). These contours suggest that along most of the interface, positive circulation is generated as the interface pressure increases from low pressure at the symmetry plane, to a higher far-field pressure. The lower-density fluid elements in the upper fluid suffer a greater inviscid acceleration towards the symmetry plane due to pressure gradients than the lower fluid, and this inviscid relative acceleration generates positive circulation in the interface. Only near the crest of the scar is the pressure gradient reversed, generating some negative circulation locally. The majority of circulation generated on the interface appears to be diffused into the upper fluid, with a comparatively smaller surface vorticity required in the lower fluid to satisfy the shear-stress balance.

While the influence of shearing vorticity in the lower fluid may be neglected for large density (dynamic viscosity) ratios, this is not the case when the density (and dynamic viscosity) ratios are smaller. As for the viscous wave, a significant portion of circulation generated on the interface must be distributed into the lower fluid, to maintain the shear-stress balance. This is illustrated by the vorticity contours for flows with $\rho_1/\rho_2 = 2$, presented in figure 22. Compared to the high-density-ratio

flow (figure 21*b*), a much larger quantity of vorticity is diffused into the lower fluid. As the shearing vorticity dominates the shear-stress balance, the flux of vorticity in the lower fluid no longer depends significantly on rotation or curvature of the interface. The $Fr = 0.1$ flow in figure 22(*b*) features a similar quantity of positive vorticity drawn away from the interface by the primary vortex as the $Fr = 0.2$ case in figure 22(*a*). This stands in contrast to the free-surface flow, where the quantity of secondary vorticity generated varies significantly with the interface curvature (Ohring & Lugt 1991).

3.4.1. *Net circulation*

Total circulation in both viscous interface and free-surface flows is constant, and equal to zero, as a consequence of flow symmetry. The vorticity field to the left of the symmetry plane is a mirror image of the vorticity on the right, providing equal and opposite contributions to the total circulation balance. Thus the total vorticity in each fluid, and total circulation in the interface, are all zero. Conservation of total circulation also follows from considering a circulation contour around the entire undisturbed far field. At a sufficiently great distance from the initial vortex pair, diffusion of vorticity across this outer boundary is negligible. Furthermore, as the far-field pressure on each side of the interface are equal, no net circulation is generated on the interface, and total circulation is conserved. This second consideration also implies the conservation of circulation for non-symmetric vortex–interface flows, such as the oblique vortex-pair interactions considered in Lugt & Ohring (1992)

Consider the reduced 'semi-infinite' circulation contour, $C$, shown in figure 20, containing all fluid to the right-hand side of the symmetry plane. Total circulation about this contour is typically not conserved due to two factors. First, vorticity may diffuse out of this contour along the symmetry plane. Loss of circulation from the right-hand contour is balanced by an equal loss of opposite-sign vorticity from the left-hand contour, with cross-diffusive annihilation of opposite-sign vorticity occurring at the symmetry plane. Second, since the interface pressure at the symmetry plane will generally differ from that at the far field, a net circulation will be generated by pressure gradients along the portion of the interface contained in $C$. An equal amount of opposite-signed vorticity is generated along the portion of the interface to the left of the symmetry plane, so net generation along the entire interface is still zero.

In terms of (2.24), we write the total circulation balance as

$$\frac{\mathrm{d}\Gamma}{\mathrm{d}t} = \int_{Sym.} \nu \hat{\boldsymbol{n}} \cdot \boldsymbol{\nabla}\omega \,\mathrm{d}s - \left[\!\left[\frac{p}{\rho}\right]\!\right]_B + \left[\!\left[\frac{p}{\rho}\right]\!\right]_A, \tag{3.14}$$

illustrating these two effects. For the free-surface case, the circulation balance (2.39) may be written

$$\frac{\mathrm{d}\Gamma}{\mathrm{d}t} = \int_{Sym.} \nu \hat{\boldsymbol{n}} \cdot \boldsymbol{\nabla}\omega \,\mathrm{d}s + \left.\frac{p_1}{\rho_1}\right|_B - \left.\frac{p_1}{\rho_1}\right|_A + \Phi_{g,1}|_B - \Phi_{g,1}|_A + \frac{1}{2}\boldsymbol{u}_1 \cdot \boldsymbol{u}_1|_B. \tag{3.15}$$

Since only the lower fluid contributes to the free-surface interface circulation, terms related to gravitational acceleration, as well as changes to the circulation integral due to stretching of the interface, appear in the total circulation balance in addition to pressure gradients.

Time histories of the circulation contained in the right half of the symmetry plane, for both free-surface and viscous interface flows, are presented in figure 23.

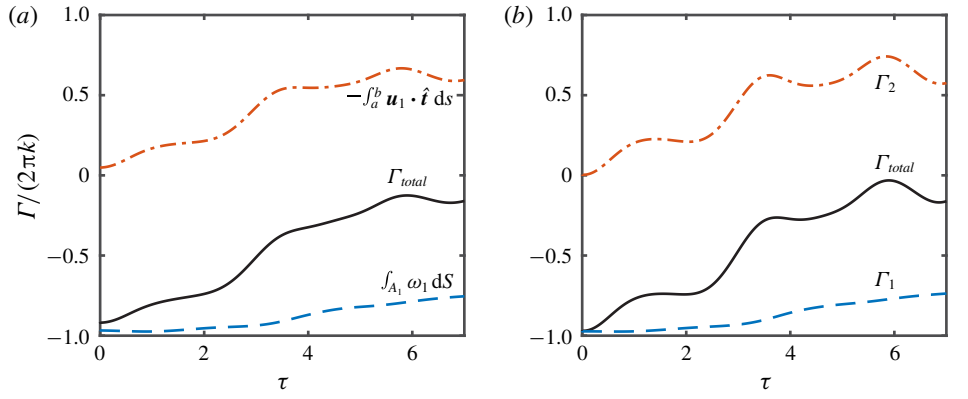


FIGURE 23. Time histories of total circulation contained in the right-hand side of the symmetry plane, for the (*a*) free-surface and (*b*) viscous interface flows presented in figure 21.

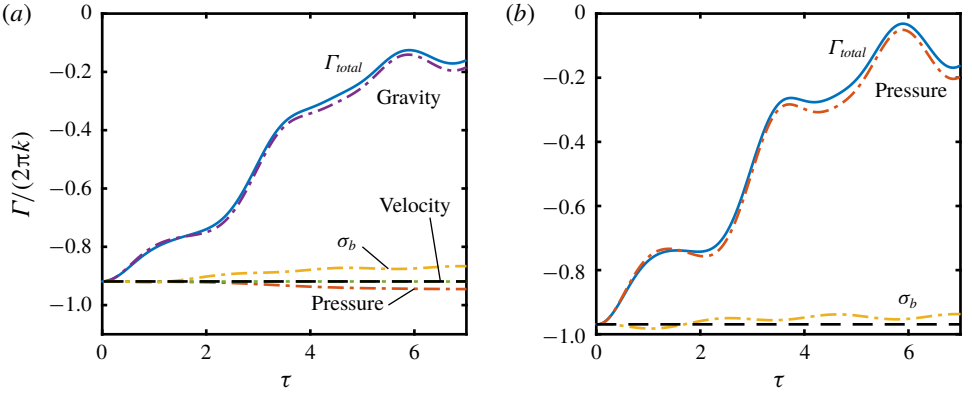


FIGURE 24. Contributions of each source term in (3.14) and (3.15) to the total circulation balance for the (*a*) free-surface and (*b*) viscous interface flows. These curves were obtained by cumulatively integrating each source term over the duration of the flow.

The viscous flow considered is that depicted in figure 21(*b*), with a density ratio of $\rho_1/\rho_2 = 100$. Strong similarities in the total circulation balance are present, demonstrating how the free-surface flow may be used to approximate viscous interfaces with large density and viscosity ratios. Initially, all circulation is found in the vortex pair, located in the lower fluid. As flow develops, the amount of negative circulation in the lower fluid decreases due to diffusion across the symmetry plane, and due to the flux of negative vorticity into, or positive vorticity out of, the interface. For the viscous interface flow, circulation in the upper fluid increases due to the flux of positive vorticity out of the interface. As the net generation on the portion of the interface contained in $C$ is not zero, the flux of vorticity out of the lower fluid does not balance the vorticity flux into the upper fluid, and the total circulation in $C$ increases (becomes less negative) throughout flow development. Figure 24(*b*) illustrates the contributions to the total circulation balance due to each source term

in (3.14). Cross-diffusive annihilation at the symmetry plane plays only a minor role, with most of the change in circulation due to pressure gradients along the interface.

For the free-surface flow, interface circulation plays a role similar to the circulation above the viscous interface. The various source terms in (3.15) generate a net positive interface circulation, as illustrated in figure 24(*a*). Some of this circulation is transferred into the lower fluid by the boundary vorticity flux, however, a large amount of the positive circulation generated remains in the interface.

While figure 23 suggests that the interface circulation is indicative of the circulation that would be found on the 'air' side of a 'free' surface, contributions from the various source terms to the generation of interface circulation in figure 24 are significantly different. The dominant source of circulation in the viscous interface is acceleration of the upper fluid due to pressure gradients. If we had used Lundgren & Koumoutsakos' description (2.36), this would also be the case for the free-surface flow (the pressure acceleration is rewritten using the transient Bernoulli equation). As our free-surface formulation ignores motion in the upper fluid, pressure accelerations are no longer the dominant source of interface circulation: gravitational acceleration of fluid elements on the free surface accounts for most of the circulation generated.

As stated previously, these 'vorticity generation' terms are a local phenomenon. Generation of vorticity to the right-hand side of the symmetry plane is balanced by equal generation of opposite-sign vorticity to the left of the symmetry plane, leading to conservation of total circulation within the flow.

#### 3.4.2. *Application to other flows*

The vortex-pair interactions presented here are for high density ratios and low Froude numbers, where deformation of the interface is fairly mild, and overturning of the free surface does not occur. Nevertheless, the generation mechanisms for vorticity in more complex flows are the same as discussed here, so long as the flow remains two-dimensional. Sarpkaya & Henderson (1984) observe two kinds of surface deformations due to a vortex pair impinging on a free surface: 'scars', which run parallel to the vortex pair; and 'striations' which lie perpendicular to the vortex pair. Dommermuth (1993) relates the appearance of striations to the formation of helical vorticity in a three-dimensional instability of the vortex pair. While the wide range of flows which are inherently three-dimensional provide a strong motivation for the formulation of a fully three-dimensional theory, it appears that even the simplest of two-dimensional free-surface flows suffer three-dimensional deformation of the interface. Extension of the present two-dimensional theory to three-dimensions is not trivial, however, preliminary research into a fully three-dimensional description of vorticity generation suggests that the inviscid relative acceleration discussed in the context of two-dimensional flows can explain all vorticity generated in three-dimensional flows. Further development of this three-dimensional theory will be the subject of a future publication.

## 4. Conclusions

We have presented a revised formulation of the generation of vorticity at generalised interfaces between incompressible, Newtonian fluids in two-dimensional flows. Importantly, we have demonstrated that normal motion of the interface is not a direct source of vorticity, and that the revised formulation enables a description of the conservation of vorticity at both stationary and deforming interfaces and free surfaces. Under the present description, the only mechanism by which a net circulation may be

generated on an interface is the inviscid relative acceleration between fluid elements on each side of the interface, due to pressure gradients or body forces. Viscous forces act to transfer circulation between the slip velocity on the interface and the fluid interior, via the boundary vorticity flux, but do not generate vorticity on the boundary. When there is no global pressure gradient or body forcing, the net rate of vorticity generation on the interface is zero, and the total circulation within the flow is constant. Local generation of vorticity is observed to occur in many cases where circulation is conserved globally.

This description does not depend on the tangential boundary conditions at the interface, and may be applied to a wide range of interfaces and boundaries, including no-slip and stress-free solid boundaries, viscous no-slip interfaces and free surfaces. At viscous interfaces, all vorticity generated at the interface is diffused into the flow by viscous forces which enforce the no-slip condition, while the distribution of vorticity across the interface is governed by the shear-stress balance. At a free surface, circulation is transferred between the interface vortex sheet and fluid elements on the free surface, to ensure that the condition of zero shear stress is maintained on the free surface.

The generation, distribution and conservation of vorticity has been demonstrated in several example flows: flat and axisymmetric stationary interfaces, periodic travelling waves on viscous interfaces and free surfaces and the interaction of a vortex pair with a free surface or viscous interface. These examples highlight the local generation of vorticity on the interface due to the inviscid relative acceleration of fluid elements, and the role of the shear-stress balance in the redistribution of vorticity across the interface. Conservation of total circulation was demonstrated in each example considered, including cases where significant deformation of the interface was observed.

## Acknowledgements

This research was supported by Australian Research Council (ARC) Discovery Grant DP170100275. This article was inspired by, and has benefited from useful discussions with, Professor M. Brøns.

## Declaration of interests

The authors report no conflict of interest.

## Supplementary movies and material

Supplementary movies and material are available at https://doi.org/10.1017/jfm.2020.128.

## REFERENCES

BATCHELOR, G. K. 1967 *An Introduction to Fluid Dynamics*. Cambridge University Press.

BOZKAYA, C., KOCABIYIK, S., MIRONOVA, L. A. & GUBANOV, O. I. 2011 Streamwise oscillations of a cylinder beneath a free surface: free surface effects on vortex formation modes. *J. Comput. Appl. Maths* **235** (16), 4780–4795.

BRØNS, M., THOMPSON, M. C., LEWEKE, T. & HOURIGAN, K. 2014 Vorticity generation and conservation for two-dimensional interfaces and boundaries. *J. Fluid Mech.* **758**, 63–93.

BROWN, D. L., CORTEZ, R. & MINION, M. L. 2001 Accurate projection methods for the incompressible Navier–Stokes equations. *J. Comput. Phys.* **168** (2), 464–499.

BUCKLEY, M. P. & VERON, F. 2017 Airflow measurements at a wavy air–water interface using PIV and LIF. *Exp. Fluids* **58** (11), 161.

BUCKLEY, M. P. & VERON, F. 2019 The turbulent airflow over wind generated surface waves. *Eur. J. Mech. (B/Fluids)* **73**, 132–143.

BULAVIN, P. E. & KASHCHEEV, V. M. 1965 Solution of the non-homogeneous heat conduction equation for multilayered bodies. *Intl Chem. Engng* **5**, 112–115.

CRESSWELL, R. W. & MORTON, B. R. 1995 Drop-formed vortex rings – the generation of vorticity. *Phys. Fluids* **7** (6), 1363–1370.

DOMMERMUTH, D. G. 1993 The laminar interactions of a pair of vortex tubes with a free surface. *J. Fluid Mech.* **246**, 91–115.

DONEA, J., HUERTA, A., PONTHOT, J.-P. & RODRIGUEZ-FERRAN, A. 2004 Arbitrary Lagrangian–Eulerian methods. In *Encyclopedia of Computational Mechanics* (ed. E. Stein, R. de Borst & T. J. R. Hughes), chap. 14. Wiley.

DOPAZO, C., LOZANO, A. & BARRERAS, F. 2000 Vorticity constraints on a fluid/fluid interface. *Phys. Fluids* **12** (8), 1928–1931.

FENTON, J. D. 1985 A fifth-order Stokes theory for steady waves. *J. Waterways Port Coast. Ocean Engng* **111** (2), 216–234.

HANSEN, A., DOUGLASS, R. W. & ZARDECKI, A. 2005 *Mesh Enhancement: Selected Elliptic Methods, Foundations and Applications*. Imperial College Press.

KÜCHEMANN, D. 1965 Report on the IUTAM symposium on concentrated vortex motions in fluids. *J. Fluid Mech.* **21**, 1–20.

LIGHTHILL, M. J. 1963 Introduction. Boundary layer theory. In *Laminar Boundary Layers* (ed. L. Rosenhead), chap. 2, pp. 46–109. Oxford University Press.

LONGUET-HIGGINS, M. S. 1953 Mass transport in water waves. *Phil. Trans. R. Soc. Lond.* A **245** (903), 535–581.

LONGUET-HIGGINS, M. S. 1960 Mass transport in the boundary layer at a free oscillating surface. *J. Fluid Mech.* **8**, 293–306.

LONGUET-HIGGINS, M. S. 1992 Capillary rollers and bores. *J. Fluid Mech.* **240**, 659–679.

LONGUET-HIGGINS, M. S. 1998 Vorticity and curvature at a free surface. *J. Fluid Mech.* **356**, 149–153.

LUGT, H. J. 1987 Local flow properties at a viscous free surface. *Phys. Fluids* **30** (12), 3647–3652.

LUGT, H. J. & OHRING, S. 1992 The oblique ascent of a viscous vortex pair toward a free surface. *J. Fluid Mech.* **236**, 461–476.

LUNDGREN, T. & KOUMOUTSAKOS, P. 1999 On the generation of vorticity at a free surface. *J. Fluid Mech.* **382**, 351–366.

MORINO, L. 1986 Helmholtz decomposition revisited: vorticity generation and trailing edge condition. *Comput. Mech.* **1** (1), 65–90.

MORTON, B. R. 1984 The generation and decay of vorticity. *Geophys. Astrophys. Fluid Dyn.* **28**, 277–308.

OHRING, S. & LUGT, H. J. 1991 Interaction of a viscous vortex pair with a free surface. *J. Fluid Mech.* **227**, 47–70.

ÖZIŞIK, M. N. 1968 *Boundary Value Problems of Heat Conduction*. International Textbook Co.

PECK, B. & SIGURDSON, L. 1998 On the kinetics at a free surface. *IMA J. Appl. Maths* **61** (1), 1–13.

PECK, B. & SIGURDSON, L. 1999 Geometry effects on free surface vorticity flux. *Trans. ASME J. Fluids Engng* **121** (3), 678–683.

REICHL, P., HOURIGAN, K. & THOMPSON, M. C. 2005 Flow past a cylinder close to a free surface. *J. Fluid Mech.* **533**, 269–296.

ROOD, E. P. 1994*a* Interpreting vortex interactions with a free surface. *Trans. ASME J. Fluids Engng* **116** (1), 91–94.

ROOD, E. P. 1994*b* Myths, math, and physics of free-surface vorticity. *Appl. Mech. Rev.* **47** (6S), S152–S156.

SARPKAYA, T. 1996 Vorticity, free surface, and surfactants. *Annu. Rev. Fluid Mech.* **28**, 83–128.

SARPKAYA, T. & HENDERSON, D. O. 1984 Surface disturbances due to trailing vortices. *Tech. Rep.* NPS-69-84-00. Naval Postgraduate School, Monterey, California.

SHERIDAN, J., LIN, J.-C. & ROCKWELL, D. 1997 Flow past a cylinder close to a free surface. *J. Fluid Mech.* **330**, 1–30.

TRUESDELL, C. 1954 *The Kinematics of Vorticity*. Indiana University Press.

TSUJI, Y. & NAGATA, Y. 1973 Stokes' expansion of internal deep water waves to the fifth order. *J. Oceanogr. Soc. Japan* **29** (2), 61–69.

WU, J. Z. 1995 A theory of three-dimensional interfacial vorticity dynamics. *Phys. Fluids* **7** (10), 2375–2395.

WU, J. Z. & WU, J. M. 1993 Interactions between a solid surface and a viscous compressible flow field. *J. Fluid Mech.* **254**, 183–211.